Western🛡Graduate&PostdoctoralStudies

Western University
Scholarship@Western

Electronic Thesis and Dissertation Repository

7-2-2020 10:10 AM

Hydrodynamic of a Novel Liquid-Solid Circulating Fluidized Bed Operating Below Particle Terminal Velocity

Xinyu Pan, *The University of Western Ontario*

Supervisor: Zhu, Jingxu, *The University of Western Ontario*
Co-Supervisor: Zheng, Ying, *The University of Western Ontario*
A thesis submitted in partial fulfillment of the requirements for the Master of Engineering
Science degree in Chemical and Biochemical Engineering
© Xinyu Pan 2020

Follow this and additional works at: https://ir.lib.uwo.ca/etd

Recommended Citation

Abstract

A novel type of circulating fluidized bed operating below the particle terminal velocity known as conventional circulating fluidized bed (CCFB) was proposed and tested for the first time in this study. The experiments were carried out in a liquid-solid circulating fluidized bed system, where both liquid and solid flew upwards in the riser and solids exiting the top of the riser were separated from liquid and then returned to the bottom of the riser via an accompanying downer. The system was essentially operated in the conventional fluidization regime but with continuously feeding of particles into riser bottom and particles moving up the riser to achieve solids circulation or circulating fluidization. The hydrodynamic of the CCFB was investigated at various operating conditions with two types of particles. The solids holdup of the conventional circulating fluidization was clearly higher when compared to conventional fluidization. Particles with a higher terminal velocity have higher solids holdup.

Keywords

Summary for Lay Audience

In chemical, biochemical and environmental processes, fluidized bed reactors are an excellent candidate for multi-phase reactions due to its good liquid-solid contact efficiency and intensified solids movement.

A new type of Liquid-Solid Circulating Fluidized Beds, called Conventional Circulating Fluidized Bed (CCFB), is conceived and tested for the first time which can be operated below the particle terminal velocity while a regular circulating fluidized bed would operate beyond the particle terminal velocity. Taking advantages of both circulating fluidized beds and conventional fluidized beds, significant dense particle population can be achieved in the CCFB. The particles represent reactant or catalyst in the fluidized bed reactor. Higher particle concentration is anticipated to result in higher reaction efficiency.

The study carried out in this thesis project focuses on the hydrodynamics of the conventional circulating fluidized bed operating at ambient temperature and pressure with particles heavier than liquid. In the CCFB, solids holdup is found to be uniform, following that of the conventional liquid-solid fluidized beds. Solids holdup is increasing with solids circulation rate and decreasing with superficial liquid velocity. It is believed that particle-particle interaction is intensified in the CCFB.

Acknowledgments

I would like to take this opportunity to express the appreciation and gratitude to those who have been helping and supporting me in the academic and daily life.

I would like to express my sincerest thanks to both Professor Jesse Zhu and Professor Ying Zheng for being my supervisors, and their guidance and extensive support through my Master's study. Thanks to their instructions and motivation, I was able to complete my research project and learn many skills at the meanwhile.

I would like to thank Professor Jesse Zhu for bringing me to Western University where I completed my Bachelor of Engineering Science degree through an exchange program. This brought me new horizon in my study as well as in my career development.

Much appreciation is extended to Tian Nan for his tremendous help during the first half of my study.

My gratefulness is also directed to all my friends for their help in the academic and daily life.

Many thanks to George Zhang for his technical support in the laboratory.

Finally, I'd like to thank my parents for their consistent and unconditional support encouragement and love. Without them, I would never make it.

Table of Contents

List of Tables

List of Figures

List of Appendices

Chapter 1

1   General Introduction

1.1   Introduction

Fluidization occurs when a fluid (liquid or gas) is pushed upwards through a bed of particle materials and causes the initially packed bed of particles to expand upwards. This makes the granular materials to behave like a liquid through suspension in a fluid that is either liquid or gas (Davidson, Clift, & Harrison, 1985; Geldart, 1986). The concept of fluidization started in 1921 by Winkler in a gas-solid coal gasification process (Winkler 1921) and later extended to liquid-solid and gas-liquid-solid three phase fluidization (Wilhelm & Kwauk, 1948). For liquid-solid fluidization, when the superficial liquid velocity is very low, the bed remains in the fixed bed state. When the liquid velocity reaches a critical value known as minimum fluidization velocity, the particles become uniformly suspended in the liquid phase and the bed material becomes fluidized. With the increase of liquid velocity, the fluidized bed would expand and the solids suspension becomes more dilute, but with a clear visible bed surface existing at the top. The liquid-solid fluidized beds facilitate excellent interactions between the solid particles and liquid phases with smooth liquid flow and uniform particle suspension. Liquid-solid fluidization has a long history in the chemical, environmental and mining industries (Epstein, 2002).

When the superficial liquid velocity in a liquid-solid fluidized bed reaches the particle terminal velocity, the particles begin to be entrained out of the bed and the bed is then transformed into a liquid-solid circulating fluidized bed where particles leaving the fluidized bed (riser column) are collected and then recycled through a solids return system, normally a downer, and fed into the bottom of the riser bed continuously. Since its inception in the 1990s, liquid-solid circulating fluidized beds (LSCFBs) have been demonstrated to have many potential applications due to their many advantages such as excellent contact efficiency between liquid and solid, high mass and heat transfer rate, easy control of large quantity of particles flow etc.(Zhu, Zheng, Karamanev, & Bassi, 2000). Applications processes of LSCFBs that have been studied included continuous

protein recovery (Lan et al., 2000), continuous enzymatic polymerization of phenol (Trivedi, Bassi, & Zhu, 2006), lactose fermentation(Patel, Bassi, Zhu, & Gomaa, 2008), biological nutrient removal from leachates (Eldyasti, Chowdhury, Nakhla, & Zhu, 2010), and wastewater treatment (Chowdhury, Nakhla, & Zhu, 2008; Nelson, Nakhla, & Zhu, 2017; Patel, Zhu, & Nakhla, 2006).

Many previous experimental and modeling studies have been carried out to investigate the hydrodynamics of liquid-solid fluidized beds in both the conventional and circulating regimes, for example, the minimum fluidization velocity(Lin, Wey, & You, 2002; Lippens & Mulder, 1993), the particle terminal velocity (Miura, Takahashi, Ichikawa, & Kawase, 2001), the bed expansion and bed voidage (Cornelissen, Taghipour, Escudié, Ellis, & Grace, 2007), the flow regimes (Liang et al., 1997; Zheng et al., 1999) and pressure balance in the system (Zheng & Zhu, 2000b). Some other factors such as heat transfer (Atta, Razzak, Nigam, & Zhu, 2009) and mass transfer (Kalaga, Dhar, Dalvi, & Joshi, 2014) have also been studied.

For a liquid-solid fluidized bed, solids holdup is an important parameter to consider when studying the hydrodynamics, as it is related to mass and heat transfer efficiency, interfacial contact efficiency and energy consumption of the fluidized bed. Higher solids holdup in conventional liquid-solid fluidized bed provides more total surface area of particles for interfacial interaction, given the higher solids holdup, but suffers from low contact efficiency between the liquid and the individual particle due to the lower slip velocity between the liquid and particles. On the other hand, circulating fluidized bed provides higher interfacial contact efficiency but suffers from low solids holdup. Therefor, it would be ideal if one can take advantages of both conventional and circulating fluidized bed and combine the features in a new type of fluidized bed.

Such new type of fluidized bed, was therefore conceived by Professor Zhu in 2016, and was tested for the first time in this Masters Project. This new type of fluidized bed is named "Conventional Circulating Fluidized Bed or CCFB" operating below the particle terminal velocity. Starting form a conventional liquid-solid fluidized bed in a fluidization column (the riser) of definite height, increasing the liquid velocity will cause the fluidized

bed to expand or the dense phase to rise while the bed or dense phase reduces its solids holdup. When the liquid velocity is sufficient, the bed level will rise to the top of the fluidization column and some particles would begin to leave should liquid velocity continue to increase. Under such condition, if particles are continuously fed into the bottom, particle circulation is realized even the superficial liquid velocity is still below the particle terminal velocity. In practice, the operation of such CCFB would be realized in a circulating fluidization system consisting a riser column (the above mentioned fluidization column), and a downer column that connects to both ends of the riser so that particles overflowing from the riser top can be recycled back to the bottom of the riser so that particles overflowing from the riser top can be recycled back to the bottom of the riser – more details to be discussed later in Chapter 3.

For the proposed conventional circulating fluidized bed (CCFB), the following advantages can be expected in comparison with the other existing liquid-solid fluidized beds.

1. Solids circulation is introduced into a conventional fluidized bed which allows for continuous operation if particles require regeneration.

2. Higher solids holdup when comparing to conventional liquid-solid fluidization and liquid-solid circulating fluidization at similar conditions.

Compared to the circulating fluidized bed (LSCFB), the significant difference between CCFB and LSCFB is that the superficial liquid velocity in CCFB is lower than the particle terminal velocity. The solids that are continuously feed into the bottom of riser and entrained out of the riser at its top then returned to the downer are the driving force required to achieve the solids circulation.

Compared to the traditional LSCFB, CCFB has a higher solids holdup under similar operating conditions. The circulation of particles below particle terminal velocity can significantly reduce energy consumption and increase contact time between the solids and liquid.

1.2 Objective

To understand the novel conventional circulating fluidization bed (CCFB) operating below the particle terminal velocity, the objectives of this research include:

1. Construct a CCFB unit and manipulate the operating conditions for achieving solids circulation under conventional fluidization.

2. Investigate the basic hydrodynamic characteristics of the CCFB, such as the solids holdup and solids circulation rate.

3. Study the effects of particle properties and superficial liquid velocity on the hydrodynamics.

1.3 Thesis Structure

This thesis contains five chapters and follows the traditional thesis format.

Chapter 1 provides a general introduction about the background and objectives of the current research as well as the thesis structure. The idea of the low velocity circulating fluidized bed called conventional circulating fluidized bed (CCFB) was proposed, where solids circulation take place while the system is operating below particle terminal velocity.

Chapter 2 gives a literature review on the conventional liquid-solid fluidization and liquid-solid circulating fluidization which covers multiple flow conditions in the area of liquid fluidization.

Chapter 3 details experiment apparatus and experimental methods of the CCFB.

Chapter 4 shows the results of the hydrodynamic of conventional liquid-solids circulating fluidized bed.

Chapter 5 gives the conclusions of this study and the recommendations for future research.

Chapter 2

2   Literature Review

2.1   The History of Fluidized Bed

Fluidization describes the process of converting a granular material from a static state to dynamic state by the passage of fluid (gas or liquid), through the empty space within this material. This process spawned the fluidized bed technology, which is useful in industries that frequently handle bulk solid material such as the petroleum industry, mineral and metallurgical industry, biological industry, etc. (Epstein, 2002).

The history of fluidization can be tracked back to the 1920s when the first fluidized bed reactor was developed by Fritz Winkler in Germany (Tavoulareas, 1991). After the success implementation of fluid catalytic cracking in 1940s, fluidization had become a new area of research in the field of chemical engineering. One of the most important developments during this period was to categorizing fluidization into two modes, based on their fluid property rather hydrodynamic behavior, gas-solid fluidization and liquid-solid fluidization, which was proposed by Wilhelm and Kwauk in 1948. They conducted experiments using a fluidized bed and revealed that a liquid-solid fluidized bed had a very homogeneous and uniform fluidization with single particles suspended by the liquid while a gas-solid fluidized bed was characterized by bubbling and slugging when the gas-solid system presented heterogeneous fluidization with the dense phase and dilute phase being clearly demarcated (Wilhelm & Kwauk, 1948). Therefore, the liquid-solid fluidization was also known as particulate fluidization and the gas-solid fluidization was known as aggregative fluidization. Comparison between gas-solid fluidization and liquid-solid fluidization is shown in Figure 2.1 (Kwauk, Li, & Liu, 2000).

Researches on fluidization had made great progress in the 1950s after a decade of knowledge and data accumulation. Richardson and Zaki, in 1954, summarized their experiment results of liquid-solid system and developed a semi empirical equation which is widely known today as the Richardson-Zaki equation (Richardson & Zaki, 1954). This equation correlated the bed viodage to superficial liquid velocity by only two parameters,

the terminal velocity of a single particle and an empirically determined exponent coefficient (n). This equation is applicable to all systems. In 1970s, several studies were carried out to research different aspects related of fluidization. On the gas-solid fluidization, classification of powder characteristics by Geldart (Geldart, 1973) was a supplement of characterize fluidization and demonstrated that the bubbling model was not sufficient to describe various fluidization. Werther (Werther & Molerus, 1973) discovered that the bubble flow rate can be maximized at a certain radial position which would also move inward as height increased. Mori and Wen (Mori & Wen, 1975) derived a formula to predict bubble size given the effect of the vessel diameter. In the same year, the fast fluidization concept was presented by Yerushalmi et. al. (Yerushalmi, Graff, Squires, & Dobner, 1976) at the Fluidization Conference in Asilomar. Around the same time, Lothar Reh (Reh, 1971) developed a concept of the circulating fluidized bed (CFB) for gas-solid reactions including calcinations, gasification and combustion. The hydrodynamics of gas-solid fluidization is still being studied to this day. On the liquid-solid fluidization, the hydrodynamic behaviors of a liquid-solid circulating fluidized bed were intensively studied by Zhu and Zheng (Zheng & Zhu, 2000b; Zheng et al., 1999; Zhu et al., 2000). Major efforts have been made to understand the particle and fluid behavior in LSCFB, and the characteristics of LSCFB.

| Fluid velocity | $< U_{mf}$ | $U_{mb} - U_{bt}$ | $U_{bt} - U_{tf}$ | $U_{tf} - U_{pt}$ | $> U_{pt}$ |

Aggregative (G/S)

gas aggregation   transition   solids aggregation

U_t
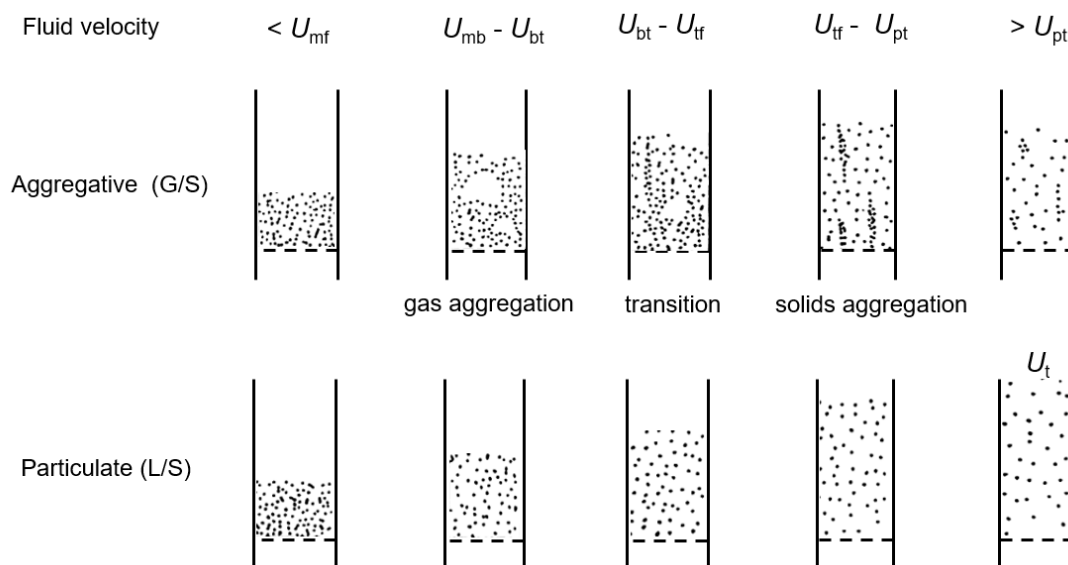
Particulate (L/S)

Figure 2.1 Comparison between aggregative fluidization and particulate fluidization (Kwauk et al., 2000)

2.2 Hydrodynamics in Conventional Liquid-Solid Fluidized Bed

2.2.1 Minimum Fluidization Velocity

Minimum fluidization velocity (U_{mf}) is defined as the minimum liquid velocity required to successfully fluidize the particles in the bed. The mechanical model explains why such velocity exists. The upward-moving liquid will exert a drag force on the other particles in the bed, and the drag force increases with liquid velocity. When the drag force balances the weight of particles, fluidization phenomenon begins to be observed. This parameter is dependent on particle density, particle size, liquid density and liquid viscosity. Based on a balance of pressure drops required to support the weight minus buoyancy acting on the particles at the point of minimum fluidization and the well-known Ergun equation, most equations for minimum fluidization velocity are in the form

$$Re_{mf} = -C_1 + \sqrt{C_1^2 + C_2 Ar} \tag{2.1}$$

where Re_{mf} and Ar are the Reynolds and Archimedes numbers given by

$$Re_{mf} = \frac{\rho_l d_p U_{mf}}{\mu} \tag{2.2}$$

$$Ar = \frac{\rho_l (\rho_p - \rho_l) g d_p^3}{\mu^2} \tag{2.3}$$

Here ρ_p, ρ_l, d_p, μ and g denote to particle and liquid density, particle diameter liquid viscosity and gravity respectively. The paired constant (C_1=33.7, C_2=0.0408) proposed by Wen and Yu have been widely used (Wen & Yu, 1966).

Based on the Ergun's equation, several simplified correlations of minimum fluidization Reynold number (Re_{mf}) had also been developed by some researchers (Babu, Shah, & Talwalkar, 1978; Bourgeois & Grenier, 1968; Richardson & da S. Jerónimo, 1979; Saxena & Vogel, 1977; Thonglimp, Hiquily, & Laguerie, 1984; Wen & Yu, 1966) to avoid the restrictions that particle sphericity and the bed voidage at minimum fluidization condition must be known in Ergun's equation. In 1985, Lucas summarized the work of these forerunners and proposed an improved equation to maximize the prediction accuracy (Lucas, Arnaldos, Casal, & Pulgjaner, 1986).

$$Re_{mf} = \left[\left(42.857 \frac{C_1}{C_2} \right)^2 + \frac{Ar}{1.75 C_1} \right]^{\frac{1}{2}} - 42.857 \frac{C_1}{C_2} \tag{2.4}$$

Studies are still ongoing. Focus is given on the correlation accuracy when applied to different particle types and different industrial applications (Anantharaman, Cocco, & Chew, 2018; Chen & Douglas, 1968).

2.2.2 Terminal Velocity and Hydraulic Transportation

Particle terminal velocity is the settling velocity of a particle in stagnant liquid at steady state. The terminal velocity of a single particle is an intrinsic characteristic of the particle,

and its calculation and measurement are as important as other intrinsic particle properties, such as particle size and density (Yang, 2003). More recent developments allow direct calculations without trial and error. The terminal velocity can be obtained by (Karamanev, 1996)

$$U_t = \sqrt{\frac{4g d_p (\rho_p - \rho_l)}{3 \rho_l C_D}} \qquad (2.5)$$

Haider and Levenspiel (1989) further suggested an approximate method for direct evaluation of the terminal velocity by defining a dimensionless particle size, d_p^*, and a dimensionless particle velocity, U^* (Haider & Levenspiel, 1989), by

$$d_p^* = d_p \left(\frac{\rho_l (\rho_p - \rho_l) g}{\mu^2} \right)^{\frac{1}{3}} \qquad (2.6)$$

$$U^* = U \left(\frac{\rho_l^2}{\mu (\rho_p - \rho_l) g} \right)^{\frac{1}{3}} \qquad (2.7)$$

Fouda and Capes (1976) also proposed polynomial equations fitted to the Heywood (1962) tables to calculate multiple terminal velocities (Fouda & Capes, 1976). The Heywood tables were widely accepted due to its simplicity and accuracy for calculating both the terminal velocity and the equivalent particle diameter. Similar types of equations were also proposed by Hartman et al. for non-spherical particles (Hartman, Trnka, & Svoboda, 1994).

2.2.3 Bed Expansion with Fluidizing Velocity

Bed expansion in liquid-solid fluidization depends on the superficial liquid velocity and the properties of the suspended particles. As the liquid flowrate increases, the packed bed transforms from packed bed into fluidized bed. As shown in Figure 2.2, bed expands with increasing superficial liquid velocity, and this trend is depicted by the curve ABCD, where AB corresponds to an fixed bed, C denotes the minimum fluidization stage, and D denotes

the maximum bed height and terminal particle velocity, above which the bed will no longer exist if no particles are fed to the bed (Leve, 1959).
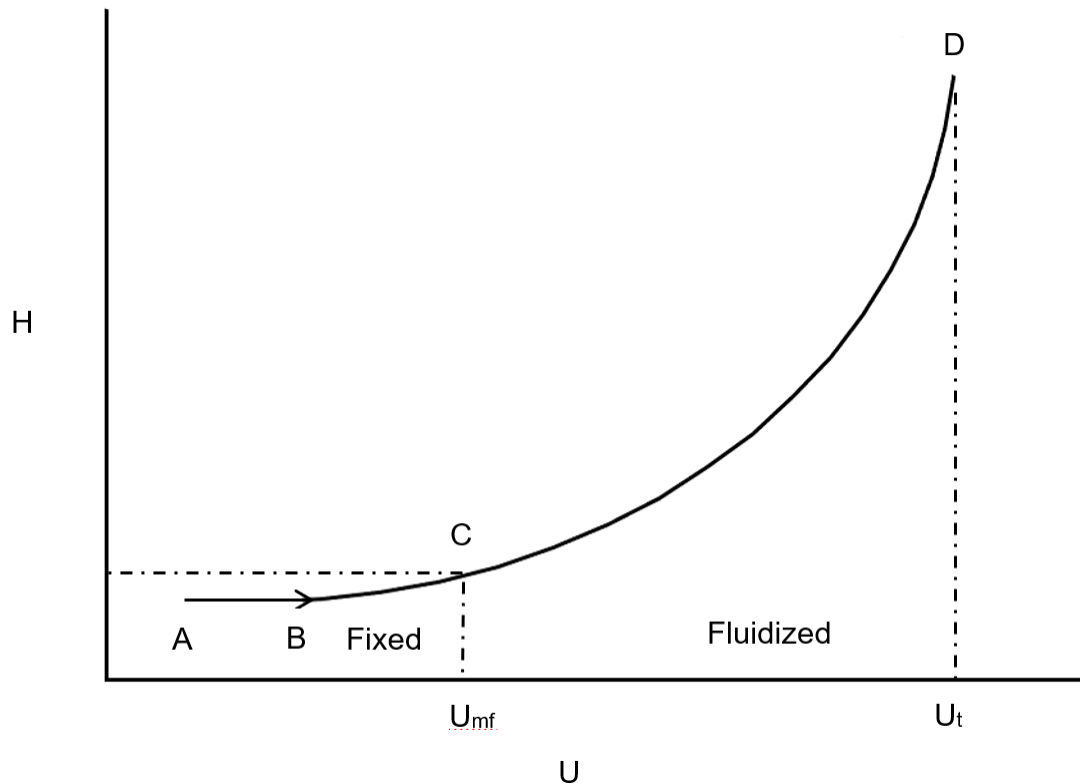
Figure 2.2 Bed height as a function of superficial liquid velocity

2.2.4 Flow Characteristics of Liquid-Solid Fluidization

Conventional liquid-solid fluidization was extensively studied in the 1950s. The Richardson and Zaki equation (Equation 2.8) has been widely applied to correlate the superficial liquid velocity and the bed voidage (Richardson & Zaki, 1954). Kwauk (Kwauk, 1963) later suggested that the concept proposed by Richardson and Zaki can also be used to characterize co-current and counter-current liquid-solid flows. The flow structure of the liquid-solid fluidization has long been described as a uniformly dispersed fluidization in both the axial and the radial directions, with or without external circulation

of particles and regardless of flow regimes (Kwauk, 1992; Wilhelm & Kwauk, 1948). This uniform behavior of a liquid-solid fluidization system makes liquid-solid fluidization an ideal system.

2.2.5 Richardson-Zaki Equation

Bed expansion is a key factor to liquid-solid fluidization study. Many of these have been discussed by Happel and Brenner and later by Jean and Fan (Happel & Brenner, 1973; Jean & Liang-Shin, 1989). A series of empirical equations proposed by Richardson and Zaki have been widely accepted due to their simplicity in use (Richardson & Zaki, 1954). The Richardson-Zaki equation dictates the relationship between bed voidage and superficial liquid velocity, given by

$$\frac{U_l}{U_t} = \varepsilon_l^n \qquad (2.8)$$

where U_l denotes superficial liquid velocity, U_t denotes particle terminal velocity, ε denotes bed voidage, and n denotes an empirically determined factor. The parameter n, can be expressed by terminal Reynolds number Re_t, and the particle to column diameter ratio, d/D. The values of parameter n are presented in Table 2.1.

Table 2.1 Values of the parameter *n* as recommended by Richardson and Zaki (Richardson & Zaki, 1954)

$n=4.65+19.5d/D$	$Re_t<0.2$
$n=(4.35+17.5d/D)\ Re_t^{-0.03}$	$0.2< Re_t <1$
$n=(4.45+18d/D)\ Re_t^{-0.1}$	$1< Re_t <200$
$n=4.45\ Re_t^{-0.1}$	$200< Re_t <500$
$n=2.39$	$Re_t >500$

Where Re_t is the terminal Reynolds number and can be expressed by

$$Re_t = \frac{U_0 d_p \rho_l}{\mu_l} \tag{2.9}$$

U_0 denotes the terminal falling velocity which can be expressed by

$$U_0 = \frac{d_p^2 (\rho_p - \rho_l) g}{18 \mu_l} \tag{2.10}$$

Many studies associated with the evaluation of the equation's accuracy and model improvement have been conducted till the present.

The Richardson-Zaki equation also indicated that the slip velocity is a function of solids holdup. Slip velocity decreases with solids holdup. The relationship between slip velocity and solids holdup is found observed which resembles the Richardson-Zaki equation in conventional fluidization

$$U_{slip} = \frac{U_l}{\varepsilon_l} = U_t \varepsilon_l^{n-1} \tag{2.11}$$

In circulating fluidization where there are solids circulation rates, the equation can be expressed by

$$U_{slip} = \frac{U_l}{\varepsilon_l} - \frac{U_s}{\varepsilon_s} = U_t \varepsilon_l^{n-1} \tag{2.12}$$

Solids holdup can be estimated through slip velocity and bed voidage.

2.3 Hydrodynamics in Liquid-Solid Circulating Fluidized Bed

2.3.1 Flow Regimes
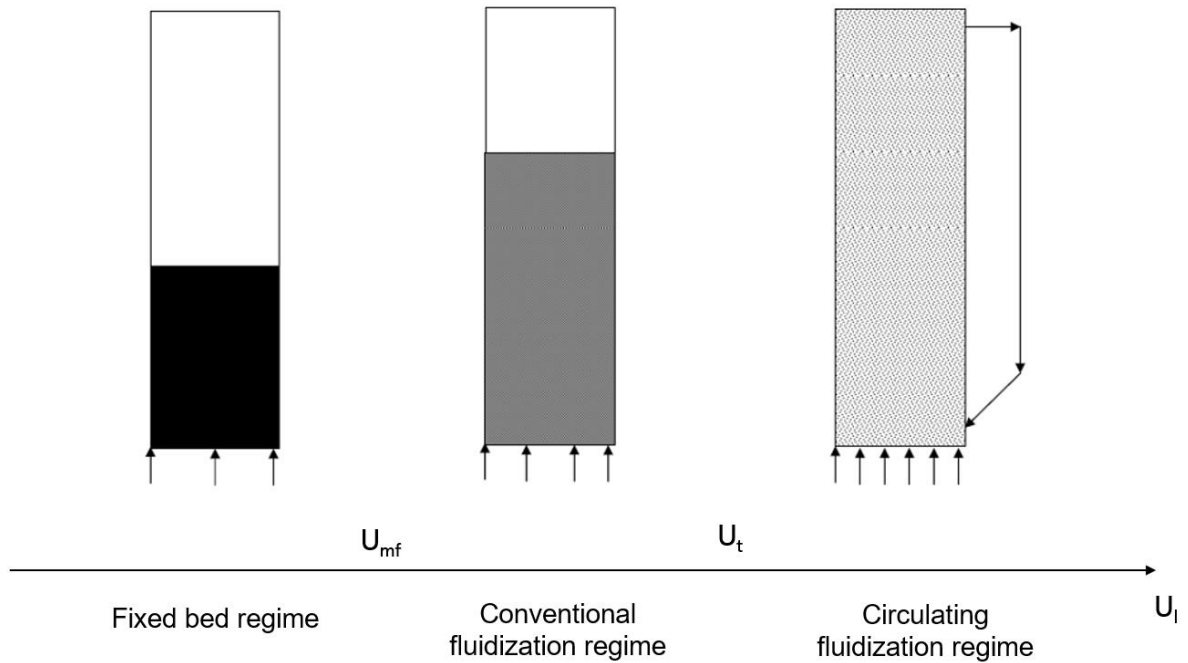
Figure 2.3 Liquid-solid fluidization flow regimes

As shown in Figure 2.3, flow regimes in the fluidization are dependent superficial liquid velocity (U_1). As superficial liquid velocity increases, the liquid-solid system experiences several flow regimes change. When superficial liquid velocity is lower than minimum fluidization velocity (U_{mf}), the bed is fixed, and the system is in the fixed bed regime. Minimum fluidization velocity is a characteristics fluidization system parameter subject to particle size, shape, density, and fluid viscosity. It marks the point at which single particles are fluidized. Therefore, as superficial liquid velocity increasing, the bed starts to expand, and particles are suspended by the liquid, that is called conventional fluidization. In conventional fluidization regime, the bed keeps expanding with increasing superficial liquid velocity until particles are entrained out of the vessel. The occurrence of

particle entrainment represents the transition from conventional fluidization to circulating fluidization. With increasing solid-liquid density ratio, the system presents more obvious transition (Liang et al., 1997; Zheng et al., 1999).
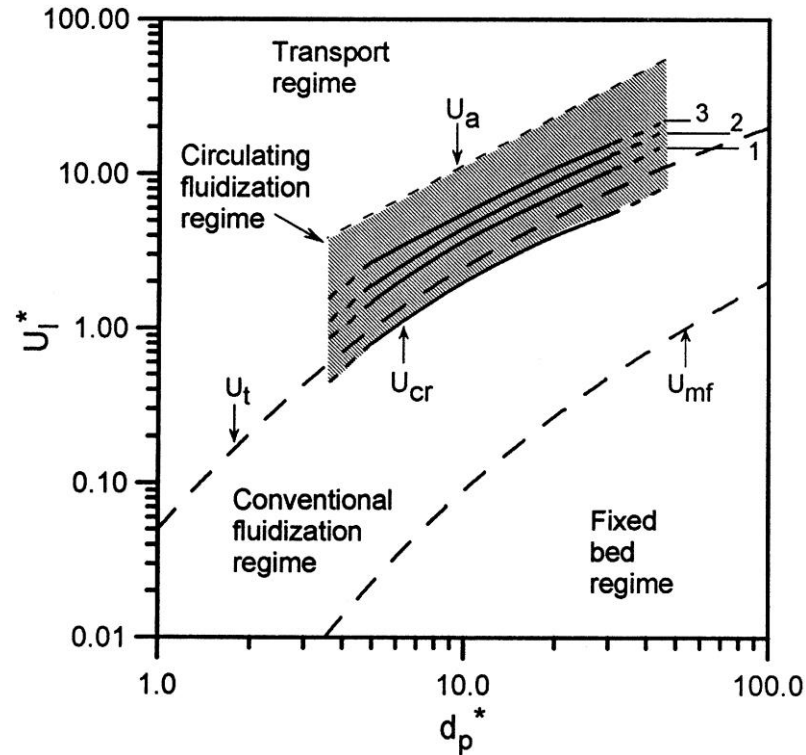
Figure 2.4 Flow regime map (Liang et al., 1997)

Many studies have reported the flow regime map of a liquid-solid fluidized bed (Sang & Zhu, 2012). With the development of liquid-solid circulating fluidized bed, the circulating fluidization regime has been added and studied extensively. As shown in Figure 2.4, the flow regime map gives a clear illustration of the boundary conditions at which flow regimes transitions from one to another in a liquid-solid fluidization system by plotting dimensionless superficial liquid velocity (U_l^*) against dimensionless particle diameter (d_p^*). These two parameters are defined with respect to superficial liquid velocity and particle size, respectively (Grace, 1986).

$$U_l^* = U_l \left(\frac{\rho_l^2}{\mu g \Delta \rho}\right)^{\frac{1}{3}} = \frac{Re}{Ar^{\frac{1}{3}}} \qquad (2.13)$$

$$d_p^* = d_p \left(\frac{\rho_p g \Delta \rho}{\mu^2}\right)^{\frac{1}{3}} = Ar^{\frac{1}{3}} \qquad (2.14)$$

The fixed bed flow regime and the conventional fluidization regime are demarcated by minimum fluidization velocity (U_{mf}), and the conventional fluidization regime and the circulating fluidization regime are demarcated by a minimum transition velocity (U_{cf}), as proposed by Liang et al. (Liang, Zhang, Yu, Jin, & Wu, 1993) and by Zheng and Zhu (Zheng et al., 1999). Later on, Zhu et al. shown that the minimum transition velocity (U_{cf}) is equivalent to the particle terminal velocity (U_t) (Zhu et al., 2000).

2.3.2 Solids Holdup

Solids holdup is one of the most important parameters of the hydrodynamics of a liquid-solid circulating fluidized bed. The solids holdup can be affected by operating conditions, such as superficial liquid velocity, auxiliary liquid velocity and solids circulation rate, as well as particle properties (Liang et al., 1997; Sang & Zhu, 2012; Zheng et al., 1999).

2.3.3 Axial Solids Holdup Distribution

The solid holdup is defined as the fraction of an element in the fluidized bed that is occupied by solid. Thus, liquid holdup, as well as bed voidage, is defined accordingly. Solid holdup and liquid holdup should satisfy $\varepsilon_s + \varepsilon_l = 1$ (Liang et al., 1997). As discussed in the flow regime section, the liquid-solid fluidization has been long considered as homogeneous in both the axial and the radial direction with or without external particle circulation and regardless of the fluidization regimes. In other words, all particles are considered to be uniformly suspended so that the radial and axial distributions of the phase holdups are uniform. The assumption of homogeneous behavior for the liquid-solid

fluidization systems considers the liquid-solid fluidization as an ideal system and forms the basis of Richardson and Zaki and Kwauk' work (Kwauk, 1963; Richardson & Zaki, 1954). Experimental results also confirm that almost all liquid-solid systems fluidized at liquid velocities below the particle terminal velocity (in the conventional low liquid velocity regime) are indeed homogeneous (Wilhelm & Kwauk, 1948).

As shown in Figure 2.5, bed height is plotted against bed voidage under various superficial liquid velocities (U_1) and their corresponding circulation rates (U_s).
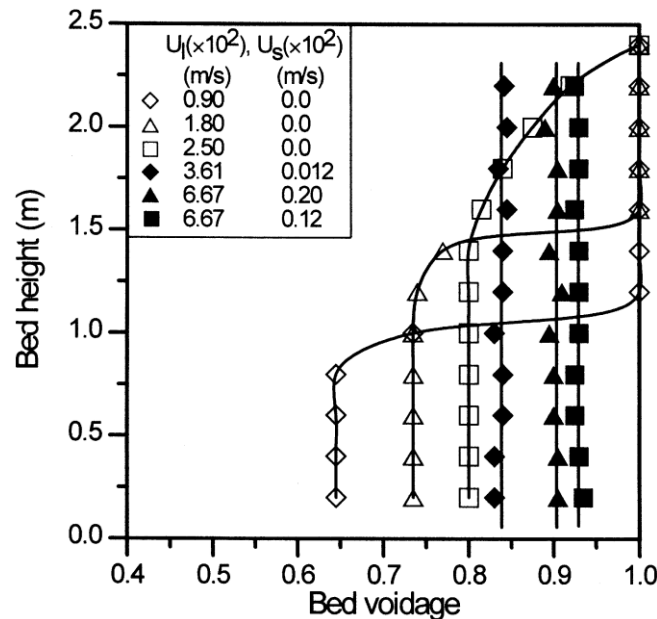
Figure 2.5 Axial liquid holdups at different positions in the conventional fluidization regime and circulating fluidization regime (Liang et al., 1997)

When $U_1 = 0.90 \times 10^{-2}$ m/s and 1.80×10^{-2} m/s, the system is in the conventional fluidization regime. The axial liquid holdups are uniform at bottom dense region, thus uniform solid holdup, and a clear distinction exists between dense phase and dilute phase. This uniformity gives conventional fluidized bed several advantages such as uniform heat and mass transfer rate, and constant contact time, which is crucial to biochemical processing (Zhu et al., 2000).

2.3.4 Radial Solids Holdup Distribution

One report by Zheng et al. (Zheng & Zhu, 2002) measured local solids holdup at seven radial positions and four axial positions of the LSCFB riser. The radial distribution of the solid holdup in the LSCFB riser is not uniform at low liquid velocities. It is thin in the center and becomes denser near the riser wall. This uneven pattern can also be observed at four different heights. At the same time, for a given liquid velocity, both the radial heterogeneity and the average solids holdup increase with the solids circulation rate. By further increasing the liquid velocity, radial non-uniformities are significantly trimmed down. This is because the flow regime has changed from circulating fluidization regime to the dilute transport regime (Liang et al., 1997). Radial heterogeneity is also related to particle density (Zheng et al., 1999). Heterogeneous distributions of solids can be measured by introducing the concepts of standard deviation and intermittent index (Brereton & Grace, 1993) and are classified as microfluidic structures (Zhu et al., 2000). These two parameters show high values in the wall area. As the solids circulation rate increases, the both parameters increase. This indicates that in both instances, the increase in solids holdup results in more variable solids motion in the wall region at higher particle circulation rates.

2.3.5 Liquid Velocity

The radial distribution of liquid velocity was only reported by few researchers (Liang et al., 1997; Zheng et al., 1999). The typical local liquid velocity is nonuniformly distributed along the radial direction, higher liquid velocity at the riser center and lower liquid velocity near the riser wall (Liang et al., 1997). By increasing the liquid velocity under the same solids circulation rate, this non-uniformity decreases because the flow regime changes from the circulating regime to the dilute transport regime(Zheng & Zhu, 2000a). Furthermore, Zheng and Zhu (Zheng et al., 1999) reported that the solids circulation rate can significantly affect the radial profile of local fluid velocity. Adding more particles leads to an increase in local liquid velocity at the axis, but a step-down at the wall. They argued that particle

concentration near the wall increases faster with increasing solids circulation rate in comparison with that at the central region (Zheng et al., 1999). To balance this variation, liquid velocity in the wall region decreases while that in the central region tends to rise. Such non-uniformity in radial liquid velocity distribution can be measured by introducing the concept of the Radial Non-uniformity Index (RNI), the normalized standard deviation of the cross-sectional average liquid velocity, which varies between 0 and 1, with larger values indicating more nonuniformity in flow structures (Zheng & Zhu, 2002).

2.3.6 Particle Velocity

Roy and his research team were the first to measure the radial distribution of particle velocity with larger particles. The increasing liquid superficial velocity steepens the radial profiles of particle velocity in the operating range of their study. It was also found that the radial profiles of particle velocity did not change significantly at the axial position (Roy, Chen, Kumar, Al-Dahhan, & Duduković, 1997; Roy, Kemoun, Al-Dahhan, & Dudukovic, 2005). Later, another group of researchers reported that the liquid distributor significantly affected the non-uniformity of the local particle velocity at the lower part of riser, however, at higher axial position, the effect of the liquid distributor became minor (Zhang, Wang, & Wang, 2003). They also investigated that the radial local particle velocity under different solids circulation rates and found that with increasing solids circulation rate, the non-uniformity of the radial local particle velocity also increased.

2.3.7 Slip Velocity

The slip velocity in LSCFB has been reported by several groups of researchers (Liang et al., 1997; Palani, Ramalingam, Ramadoss, & Seeniraj, 2011; Zheng et al., 1999), who also found that the calculated apparent slip velocity was larger than the calculated average slip velocity based on the Kwauk's theory (Kwauk, 1963), which is valid for the conventional

fluidization regime. In order to improve the existing correlations, Palani et. al. and Sang and Zhu proposed two mathematical correlations to predict the average slip velocity independently (Palani et al., 2011; Sang & Zhu, 2012). However, all the mentioned studies above investigated the average slip velocity only.

2.3.8 Modeling

Researches on LSCFB modelling are studied via two approaches, analytical method and numerical method. The analytical method is based on fluid dynamics, classic correlations and assumptions while the latter is based on computational fluid dynamics (CFD). In addition, artificial neural networks was developed to model and study the phase holdup distribution of LSCFB systems (Razzak, Rahman, Hossain, & Zhu, 2012). A simple one-dimensional models can be used to predict solids holdups and slip rates of homogeneous fluidization(Kwauk, 1963; Richardson & Zaki, 1954). However, it was found that this one-dimensional model is ineffective due to the uneven radial distribution under circulating flow conditions (Liang et al., 1997). To predict this heterogeneity, a cyclical core model was proposed to investigate this heterogeneity (Liang & Zhu, 1997). In this type of model, the riser is divided into two parts. The central core area and the annular area next to the wall. Within each zone, it is assumed that the fluidization is uniform and the flow conditions (liquid and solid residue, particle and liquid velocity, etc.) are assumed to be constant. Radial inhomogeneities are resolved by flow separation between the two regions. This model can predict the average solids, liquid velocity, particle velocity, and slip velocity for each region under different operating conditions. One limitation of this model is that the predictions are still based on averages and cannot provide an accurate radial profile. In order to overcome this limitation, methods based on the drift flow model predict the experimentally observed flow phenomena at the expense of introducing an additional empirical parameter called the distribution coefficient (Palani, Velraj, & Seeniraj, 2007).

For the numerical calculations approach, Roy and Dudukovic (Roy & Dudukovic, 2001), based on the CFD two-fluid Euler-Lagrange model, simulated the residence time

distribution of liquids and solids in risers as well as the solids velocity and the retention modes. The experimental results were validated the predictions and shown the application in predicting the degree of solids back-mixing in a reactor. Next, Cheng and Zhu (Cheng & Zhu, 2005) created a CFD model based on the two-stage Eularian-Eularian method and the hydrodynamics of the LSCFB riser under different operating conditions, different particle properties and different riser sizes was simulated. The model predictions are in good agreement with the experimental data in the literature. In addition, the simulation results provide solid retention at each axis position, a detailed radial distribution of the liquid and particle velocities, and turbulence intensities that are difficult to measure experimentally. Later, the same research group examined the LSCFB expansion problem using a CFD model and compared it with similar methods. Their studies show that combining reliable CFD models with appropriate simulation amplification can result in better reactor design, amplification, and operation (Cheng & Zhu, 2008).

2.4   Liquid-Solid Fluidization Applications and Perspectives of CCFB

Liquid-solid fluidization has a long history and wide applications. The applications of liquid-solid fluidization include particle classification, leaching and washing, adsorption and ion exchange, liquid-solid fluidized bed heat exchanger and liquid-solid fluidized bed bioreactor (Epstein, 2002).

Under similar operating conditions, CCFB have the higher solids holdup compared to the traditional LSCFB. The feasibility of operating the circulating fluidized bed below particle terminal velocity can significantly lower the energy consumption and increase the liquid-solid contact time in comparison with traditional liquid-solid circulating fluidization. Lower liquid velocity in fluidized bed means that it takes less energy to convert it into kinetic energy. In addition, as liquid moves fast in the fluidized bed, particles will accelerate accordingly. Therefore, particles are more easily to be entrained out of the bed which means less contact time.

Chapter 3

3 Experiments Apparatus and Methods

3.1 Particle Properties

All experiments were carried out at ambient temperature. Tap water was used as the fluidizing liquid. Particle which has heavy density than water was selected for upflow fluidization. One objective of this study is to investigate the effects of particle properties on hydrodynamic of liquid-solid circulating fluidized bed. Various types of particles with a wide span of densities and diameters were preferred. Unfortunately, glass beads that are 1000 - 1300 µm in diameter cannot be circulated due to the small diameter of column.

Three types of particles were used in this study and their properties are listed in Table 3.1. The average equivalent diameter was calculated from particle size distribution. Size distribution was measured from 1.0 kg particle by sieves. The minimum fluidization velocities were measured during the experiments. The particle terminal velocity, U_t, can be calculated from the following equations (Karamanev, 1996):

$$U_t = \sqrt{\frac{4gd_p(\rho_p - \rho_l)}{3\rho_l C_D}} \tag{3.1}$$

$$C_D = \frac{432}{Ar}\left(1 + 0.0470Ar^{\frac{2}{3}}\right) + \frac{0.517}{1 + 154Ar^{-\frac{1}{3}}} \tag{3.2}$$

Table 3.1 Particle properties

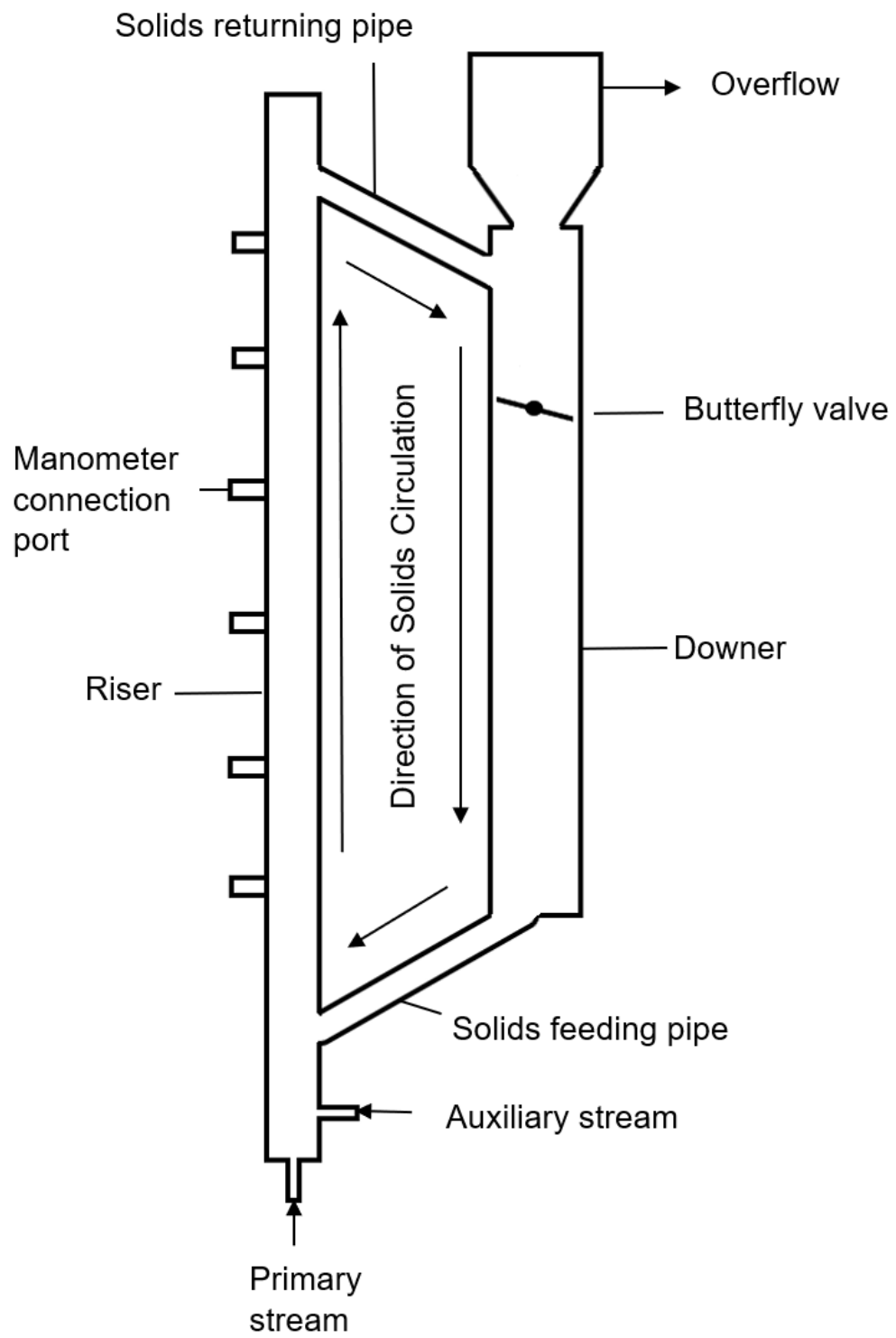| Particles	Density ρ_p (kg/m³)	Diameter d_p (µm)	Minimum fluidization velocity U_{mf} (cm/s)	Terminal velocity U_t (cm/s)
Plastic beads (PB)	1271	725	0.10	8.8
Plastic beads (PB)	1321	525	0.07	5.6

3.2 Experimental Apparatus

Figure 3.1 The schematic diagram of CCFB apparatus

The set-up of CCFFB system is shown schematically in Figure 3.1. The system consists of a 0.032m ID riser column, where the upflow fluidization takes place, a 0.051m ID downer column, and a 0.064m ID column with butterfly valve for measuring the solids circulation rate at the top of downer. The riser is connected to the downer column through the solids returning pipe at the top and the solids feeding pipe at the bottom. There are two distributors: the main liquid distributor made of a brass tube and extending 0.1 m into the riser, and the auxiliary liquid distributor made of a brass tube at the bottom of riser. Main liquid distributor is located higher than the solids feeding pipe, but the auxiliary liquid distributor is located below the solids feeding pipe thus it can control solids circulation rate.

Starting with an initial solids inventory height in the downer, the system is operated under conventional fluidization regime, where there is a clear boundary between the particle suspension and the freeboard. The bed expansion is controlled by superficial liquid velocity. At steady state, the height of expansion in the conventional fluidized bed would match the height of solids inventory in downer, as extra particles are transported into riser when the downer reaches steady state. With conventional fluidization as an initial state, increasing auxiliary flowrates as to feed particles would transfer the bed into conventional circulating fluidization while keeping the superficial liquid velocity in the riser constant.

With such a configuration, particles introduced into the riser bottom are carried up to the top of the riser by the combined liquid flow (the primary liquid flow plus the auxiliary liquid flow) and separated at the top of downer. Liquid is then returned to the liquid reservoir for reuse while the particles are returned to the downer column after passing through the solids circulation rate measuring device and re-introduced into the riser via the solid feeding pipe to re-fluidize. Therefore, the particles are continuously circulating inside the CCFB system.

The liquid flow rate and solids circulation rate can be controlled independently by adjusting the primary and the auxiliary liquid flow rates. The auxiliary liquid stream controls the quantity of the particles recirculating from the downer to the riser: when the

auxiliary flow is set to zero, no particles can enter the riser and no continuous particle circulation could be formed. Introducing the auxiliary liquid flow, solids do not begin to flow immediately. Only when the auxiliary liquid flow reaches a threshold flow rate, solids begin to flow. After that, additional liquid added to the riser cause more particles to enter the riser.

3.3 Measurement Methods

Key parameters measured in this study including average solids holdup (ε_s) and solids circulating rate (U_s). Their corresponding measuring devices are listed in Table 3.2.

Table 3.2 Measurement methods for different parameters

Parameters	Measuring devices
Average solids holdup	Manometer
Solids circulation rate	Butterfly valve

The average solids holdup (ε_s) is obtained from the measurement of pressure drop with manometers. Six pressure ports are installed along the riser column and connected to six manometers respectively to obtain the pressure at different riser heights. Since the hydrostatic pressure at different heights of riser column was high, open-end manometers were not used in this study to prevent the overflowing of water in manometers. In this experiment, the ends of manometers were connected to a tank full of air and the pressure of air inside the tank can be controlled. The sampling positions on axial directions are 27, 108, 186, 264, 324 and 385cm away from the main liquid distributor. With the following equation, the average solids holdup can be calculated based on the pressure drop due to the density difference between the particles and fluidization liquid:

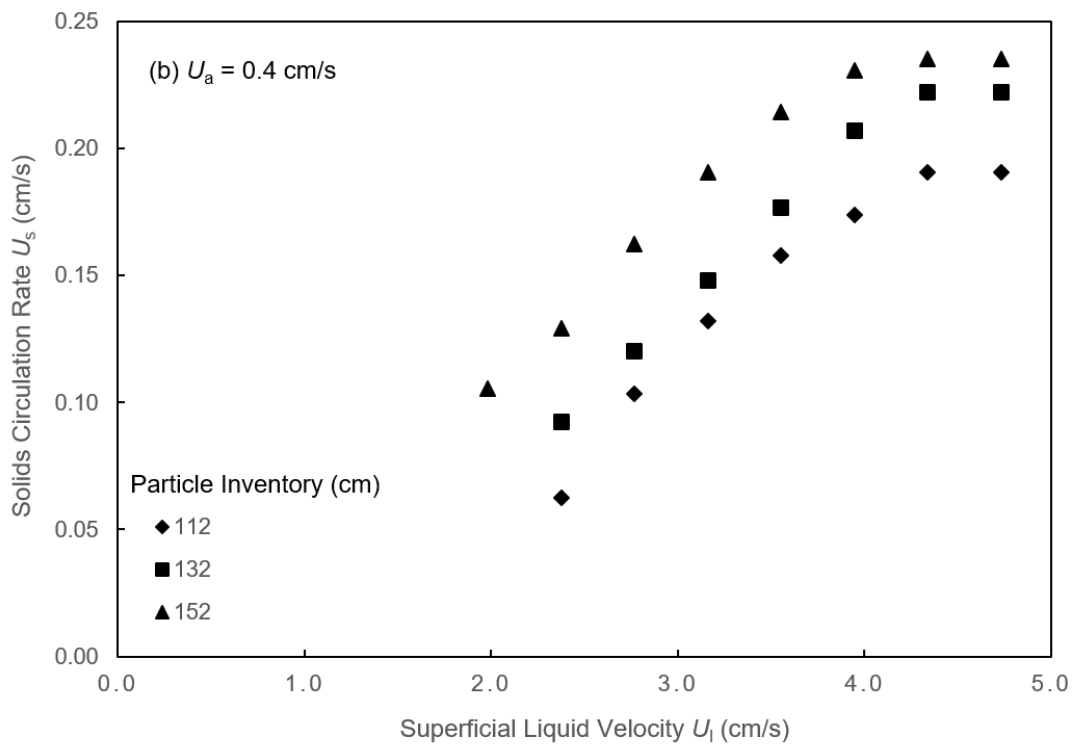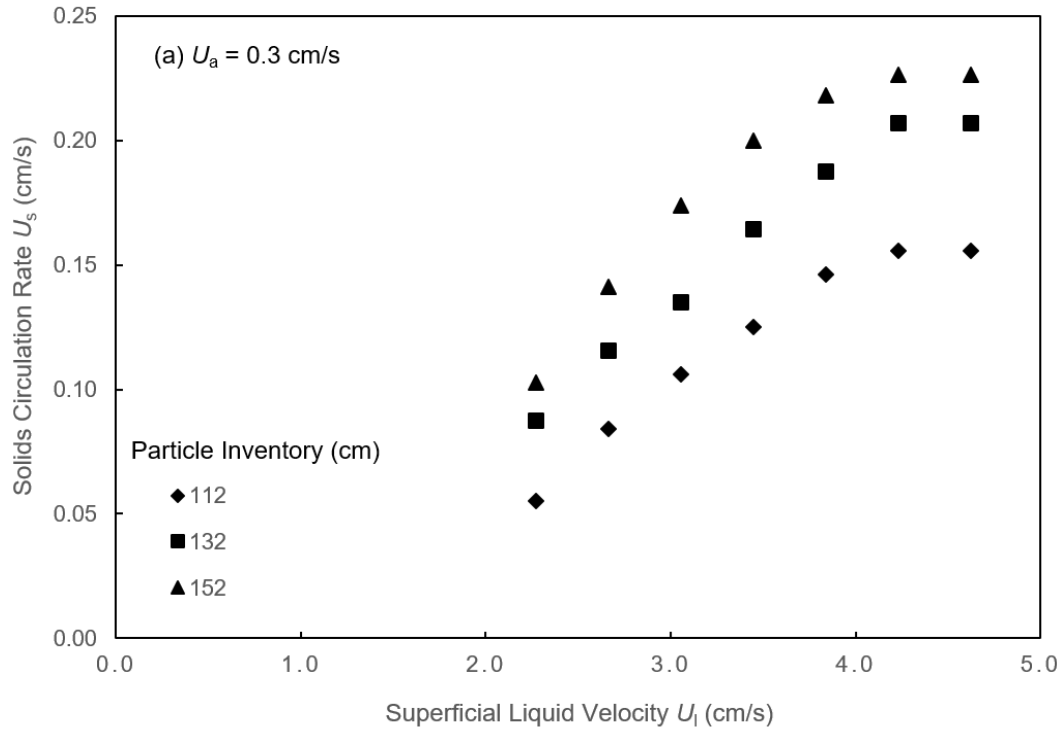$$\varepsilon_s = \frac{\rho_l \Delta h}{(\rho_p - \rho_l)\Delta H} \tag{3.3}$$

where Δh is the water level difference between two manometers, ΔH is the height difference between two probes.

3.4 Measurement and Control of Solids Circulation Rate

Solids circulation rate is used to characterize the flowrate of solids in the circulating fluidized bed. In liquid-solid systems the superficial solid velocity (U_s, m/s) is commonly used (Liang et al., 1997). Solids circulation rate is controlled by the auxiliary liquid velocity. For a constant auxiliary liquid velocity, solids circulation rate is increasing with total superficial liquid velocity. Beyond the turning point, solids circulation rate is limited by the pressure drop between the storage column and liquid flow distributor dictated by auxiliary flowrate (Zheng et al., 1999).

Solids circulation rate can be measured by the butterfly valve as shown in Figure 3.1. By closing the butterfly valve, all falling particles are collected and increase the packed bed height with time elapsing. A certain distance from the closed valve is marked with a line. Once the particles bed surface passes the line, the accumulative time is recorded. The solids circulation rate can be calculated by knowing the time period for solids accumulation, the solids packed height and riser cross-section area.

Figure 3.2 shows the effects of particles inventory (initial bed height in downer) on the solids circulation rate. With increasing particles inventory and/or auxiliary liquid velocity, the solids circulation rate increases. These figures present the relationship between particles inventory and solids circulation rate, thus the solids circulation rate can be easily controlled.

(a) U_a = 0.3 cm/s

Solids Circulation Rate U_s (cm/s)

Particle Inventory (cm)
◆ 112
■ 132
▲ 152

Superficial Liquid Velocity U_l (cm/s)

(b) U_a = 0.4 cm/s

Solids Circulation Rate U_s (cm/s)

Particle Inventory (cm)
◆ 112
■ 132
▲ 152

Superficial Liquid Velocity U_l (cm/s)
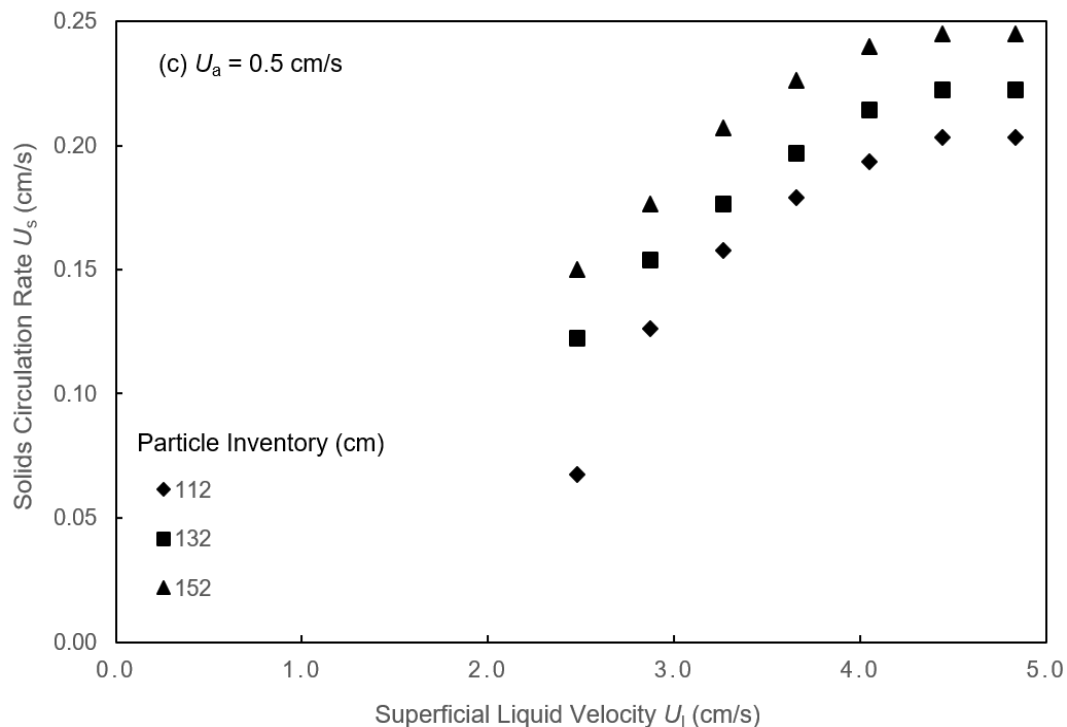
Figure 3.2 Solids circulation rate (U_s) vs. superficial liquid velocity (U_l) at different particle inventory (initial bed height in downer) for PB725 with different auxiliary liquid velocity (U_a) of (a) 0.3 cm/s, (b) 0.4 cm/s and (c) 0.5 cm/s

3.5 Accuracy of Analysis

In order to ensure the accuracy of solids holdup, preliminary measurements and analyses of standard error were accounted for PB725. For seven different superficial liquid velocities, three measurements were taken for each superficial liquid velocity. The error bar of solids holdup is shown in Figure 3.3. According to the figure, the error bar is small and it is shown that the measurement is reliable.

Figure 3.3 Solids holdup (ε_s) versus superficial liquid velocity (U_l) with error bar for PB725

Chapter 4

4   Results and Discussion

Experiments to investigate the hydrodynamics of PB525 and PB725 in conventional
fluidization and conventional circulating fluidization were operated at various conditions
in the prescribed column in Chapter 3. The performance of a fluidized bed unit is directly
associated with solids holdup, which is an indication of liquid-solid contact intensity and
efficiency. The primary liquid velocity and auxiliary liquid velocity were the parameters
to control solids circulation rate and therefore solids holdup. A higher solids holdup can
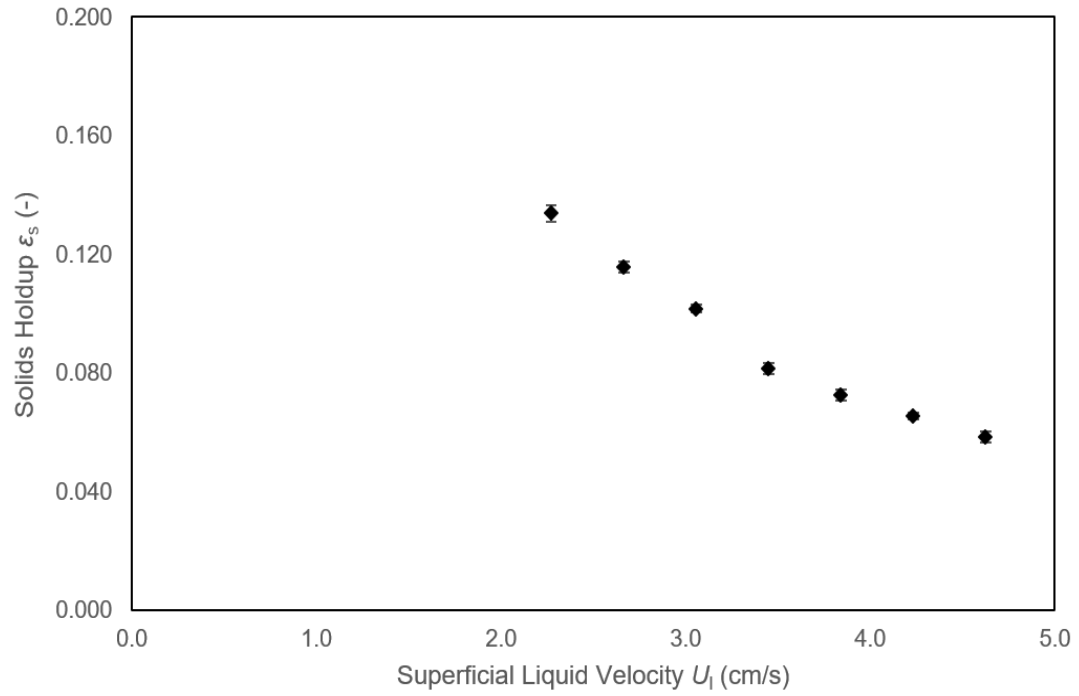be observed in conventional circulating fluidization comparing to conventional
fluidization.

4.1   Conventional Fluidization

The conventional fluidization of PB525 and PB725 were achieved with the superficial
liquid velocity increasing from 0.8 cm/s to around 4.0 cm/s for PB525 and 5.0 cm/s for
PB725. The relationship between solids holdup and superficial liquid velocity for PB525
and PB725 is shown in Figure 4.1. It could be found that solids holdup decreases with
superficial liquid velocity and such decrease becomes slower at higher superficial liquid
velocity for both PB525 and PB725. When the superficial liquid velocity increased to 4.0
cm/s, the solids holdup for PB525 became very dilute and approached zero. For PB725,
when the superficial liquid velocity reaches around 5.0 cm/s, the solids holdup was also
approaching zero.
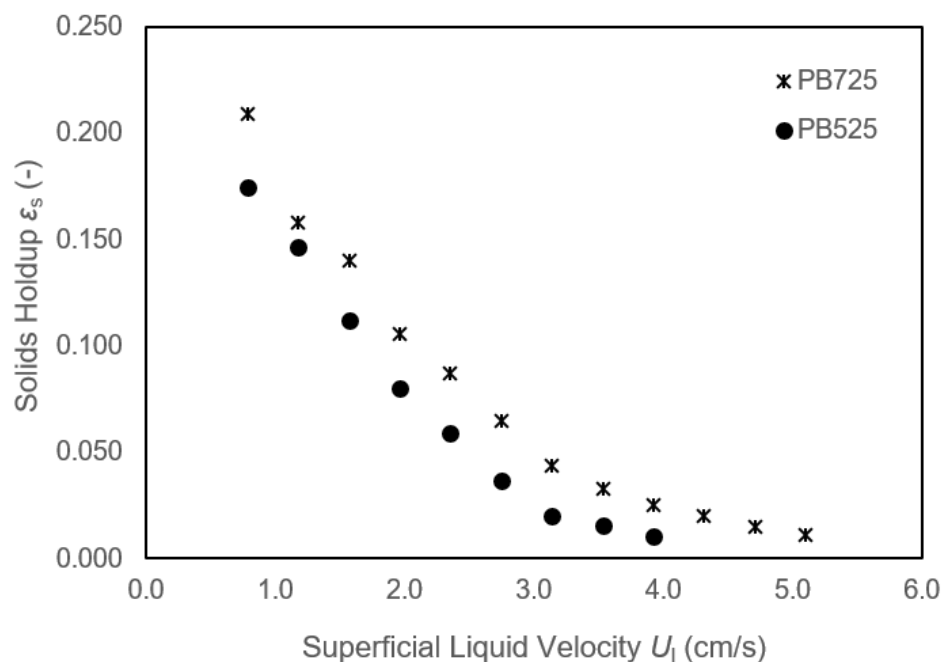
Figure 4.1 The relationship between solids holdup (ε_s) and superficial liquid velocity (U_l) for PB525 and PB725 in conventional fluidization regime

4.2 Conventional Circulating Fluidization

Knowing the solids holdup distribution is crucial in designing a fluidized bed reactor, as the same average solids holdup but different axial solids holdup distribution may result in different performance. The studies on conventional circulating fluidization of PB725 were carried out at the conditions of constant superficial liquid velocity with varying solids circulation rate or constant solids circulation rate with varying superficial liquid velocity.

(a) U_l = 2.4 cm/s   PB725

U_s (cm/s)
● 0.07
■ 0.09
♦ 0.12
▲ 0.15
✳ 0

Height (cm)

Solids Holdup ε_s (-)

(b) U_l = 3.2 cm/s   PB725

U_s (cm/s)
● 0.09
■ 0.13
♦ 0.18
▲ 0.22
✳ 0

Height (cm)
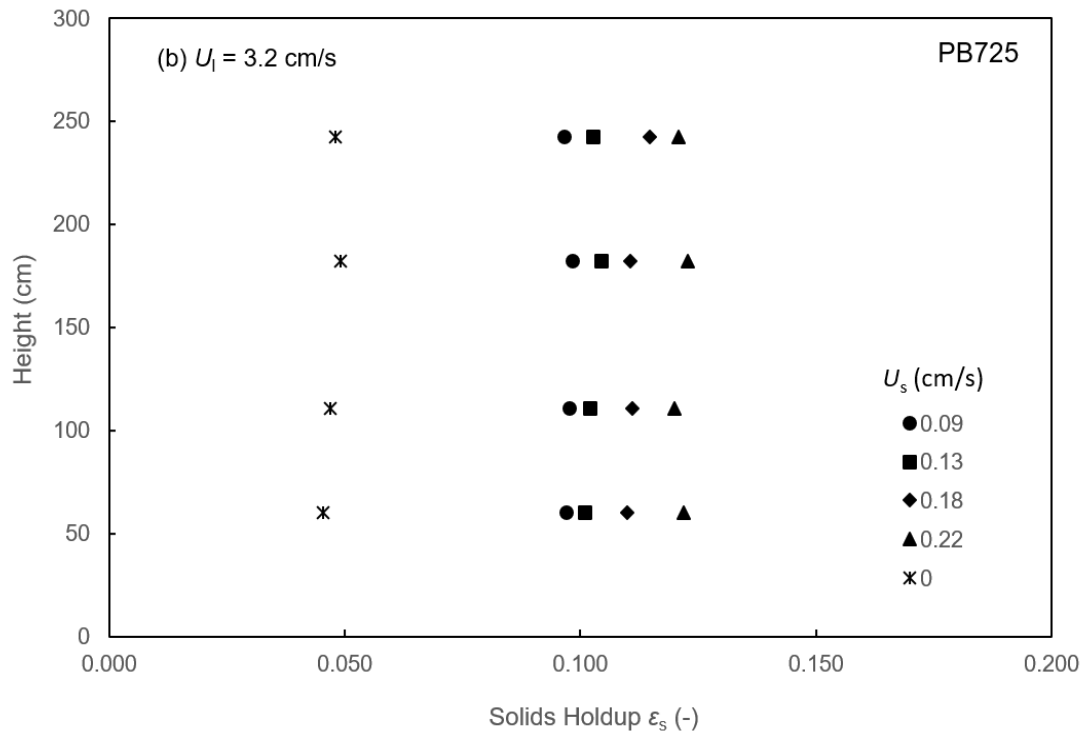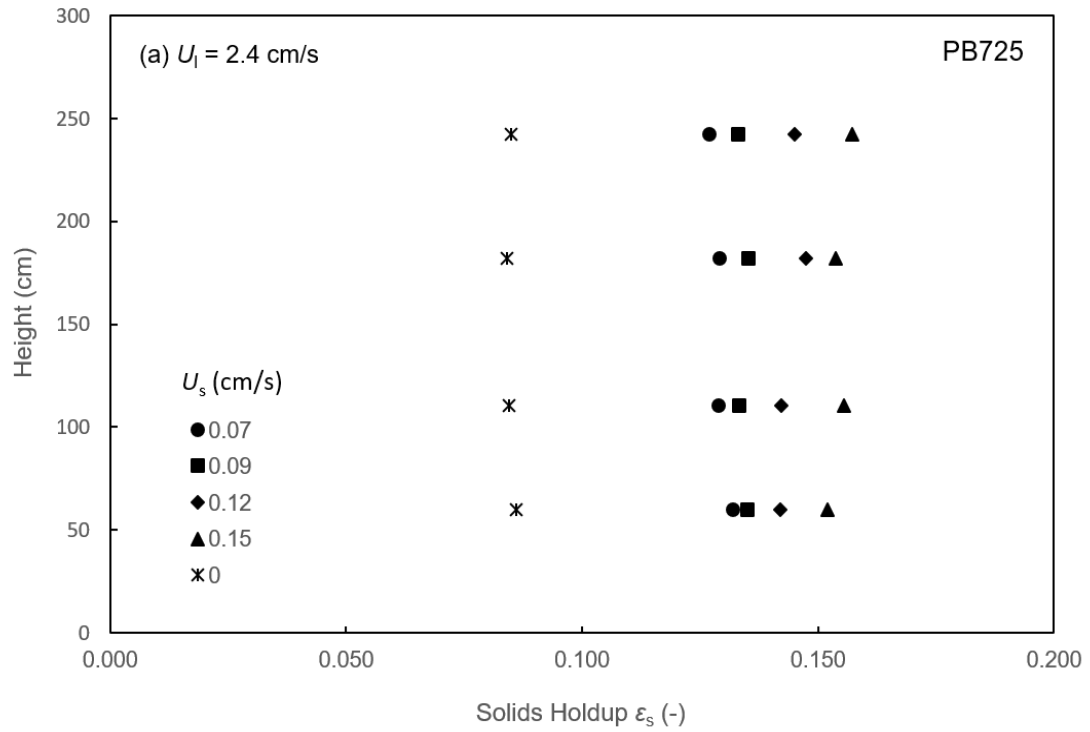
Solids Holdup ε_s (-)

Figure 4.2 Axial solids holdup distribution for PB725 under different superficial liquid velocity (U_l) (a) 2.4 cm/s, (b) 3.2 cm/s, (c) 3.9 cm/s and (d) 4.7 cm/s

Figure 4.2 shows the axial solids holdup distribution for PB725 under four constant superficial liquid velocities, 2.4 cm/s, 3.2 cm/s, 3.9 cm/s and 4.7 cm/s, with varying solids circulation rate. The data were collected at four different axial locations along the riser column by manometers. The axial solids holdup distribution for PB725 in conventional fluidization was also included in Figure 4.2 for comparison purpose. For a constant superficial liquid velocity, higher solids holdup could be obtained for PB725 with increasing solids circulation rate. Under the constant superficial liquid velocity, increasing the solids circulation rate made the axial solids holdup more uniform. It was uniform through the riser at the highest operating solids circulation rate for each corresponding velocity. Compared to the conventional fluidization, conventional circulating fluidization had the higher solids holdup under the same superficial liquid velocity and the axial solids holdup distribution becomes more uniform with the help of solids circulation. With the increase of superficial liquid velocity, the solids holdup decreased.

Figure 4.3 Axial solids holdup distribution for PB725 under different solids circulation rate (U_s) (a) 0.13 cm/s, (b) 0.18 cm/s and (c) 0.22 cm/s

The axial solids holdup distribution for PB725 under three different constant solids circulation rates, 0.13 cm/s, 0.18 cm/s and 0.22 cm/s, with varying superficial liquid velocities is shown in Figure 4.3. The data were collected at four different axial positions. For a constant solids circulation rate, increasing superficial liquid velocity decreased the solids holdup. It was uniform through the riser at the highest operating superficial liquid velocity for each corresponding solids circulation rate. As the solids circulation rate increased, the effect of superficial liquid velocity on solids holdup increased.
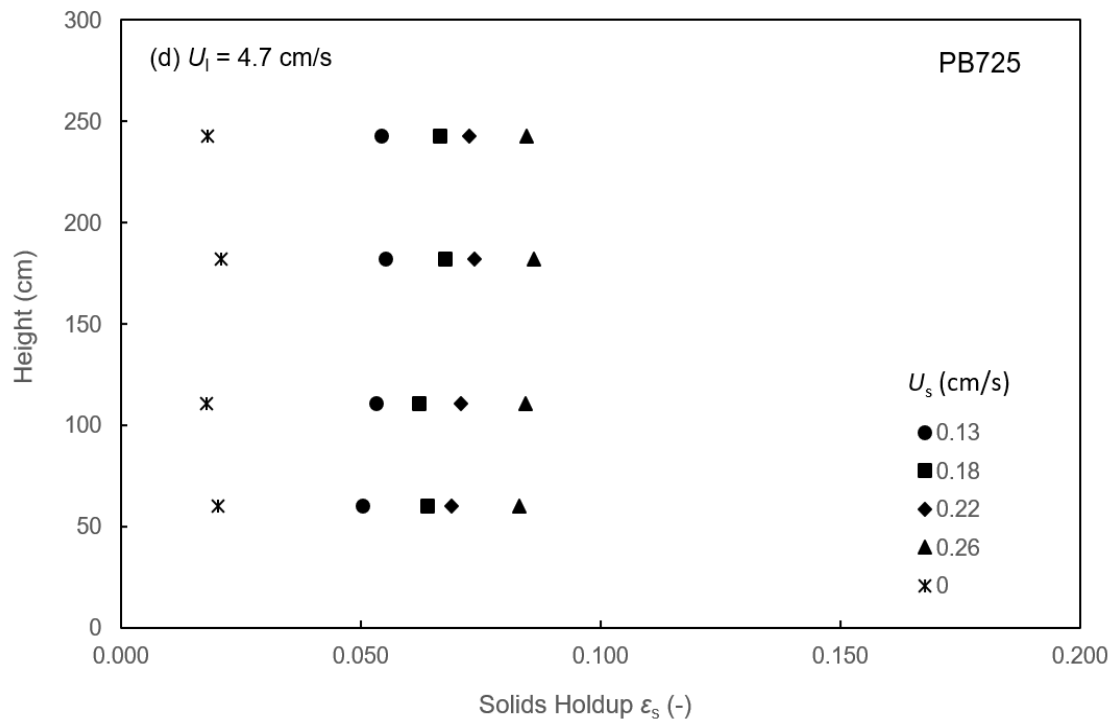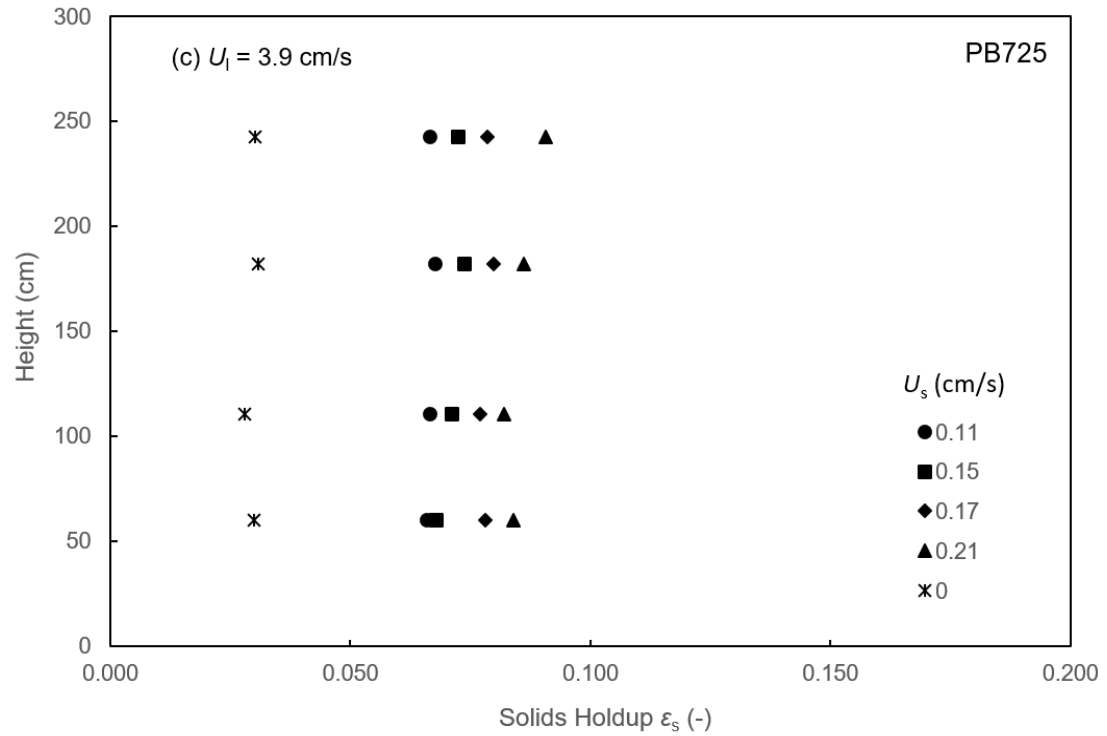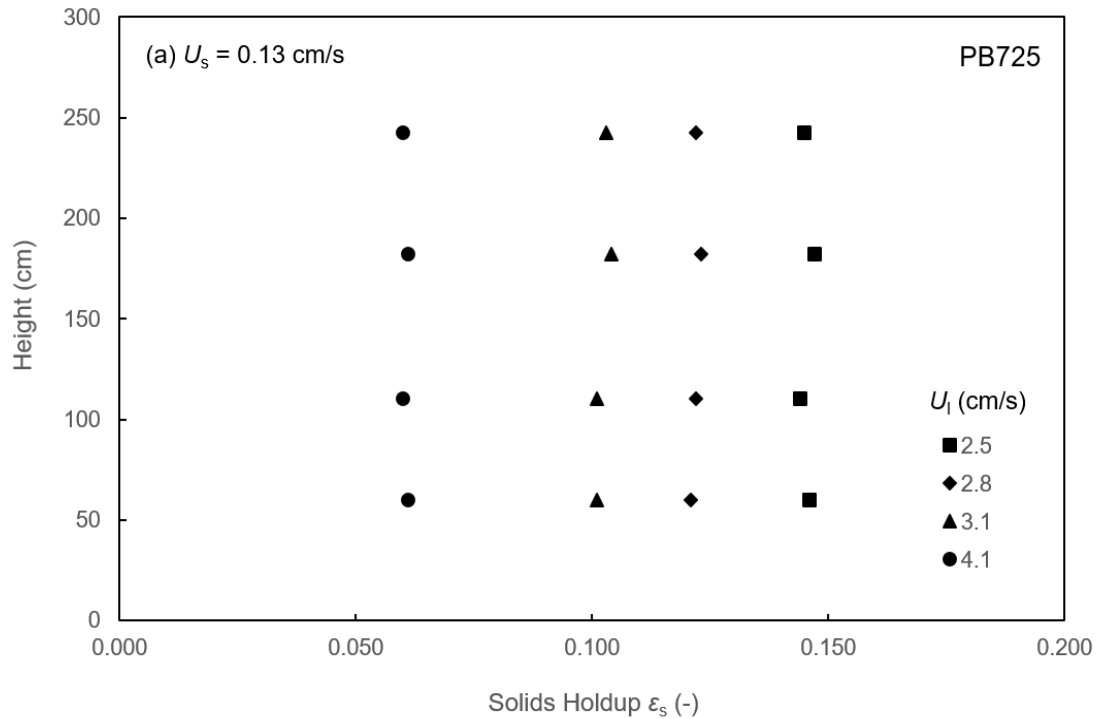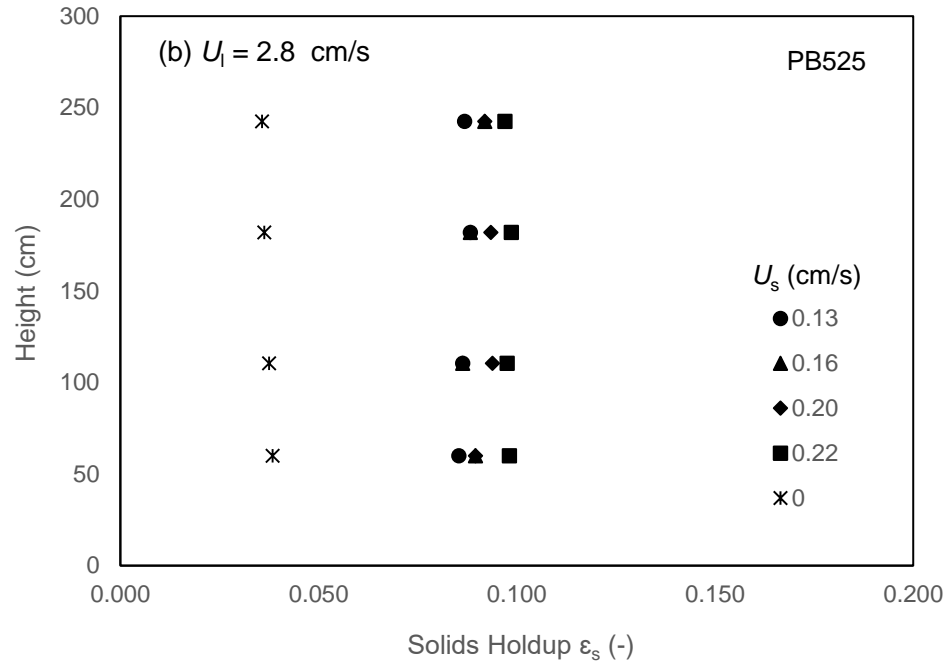
Figure 4.4 Axial solids holdup distribution for PB525 under different superficial liquid velocity (U_l) (a) 2.0 cm/s, (b) 2.8 cm/s and (c) 3.6 cm/s

Figure 4.4 shows the axial solids holdup distribution for PB525 under three different constant superficial liquid velocities, 2.0 cm/s,2.8cm/s and 3.6 cm/s, with varying solids circulation rate. The data were collected at four different axial height. The axial solids holdup distribution for PB525 in the conventional fluidization was also included in Figure 4.2. For a constant superficial liquid velocity, solids holdup increased with increasing solids circulation rate. Under the constant superficial liquid velocity, increasing the solids circulation rate made the axial solids holdup more uniform. It was almost uniform through the riser at the highest operating solids circulation rate for each corresponding velocity. Compared to the conventional fluidization, conventional circulating fluidization had a higher solids holdup under the same superficial liquid velocity and the axial solids holdup distribution became more uniform with the help of solids circulation.
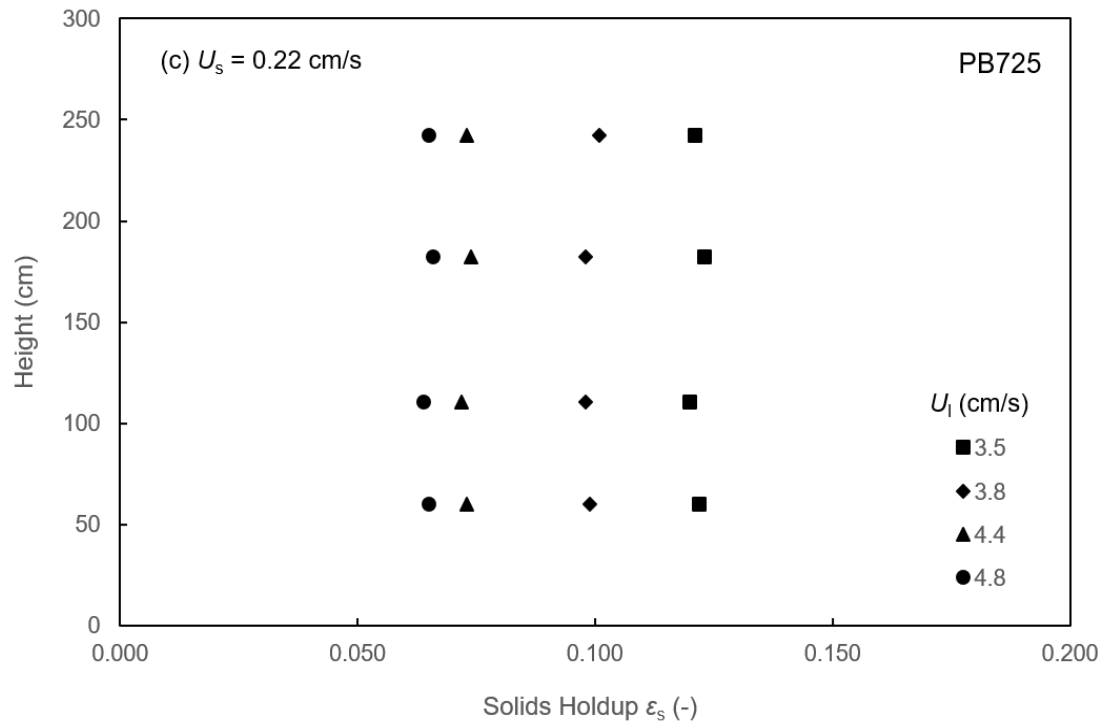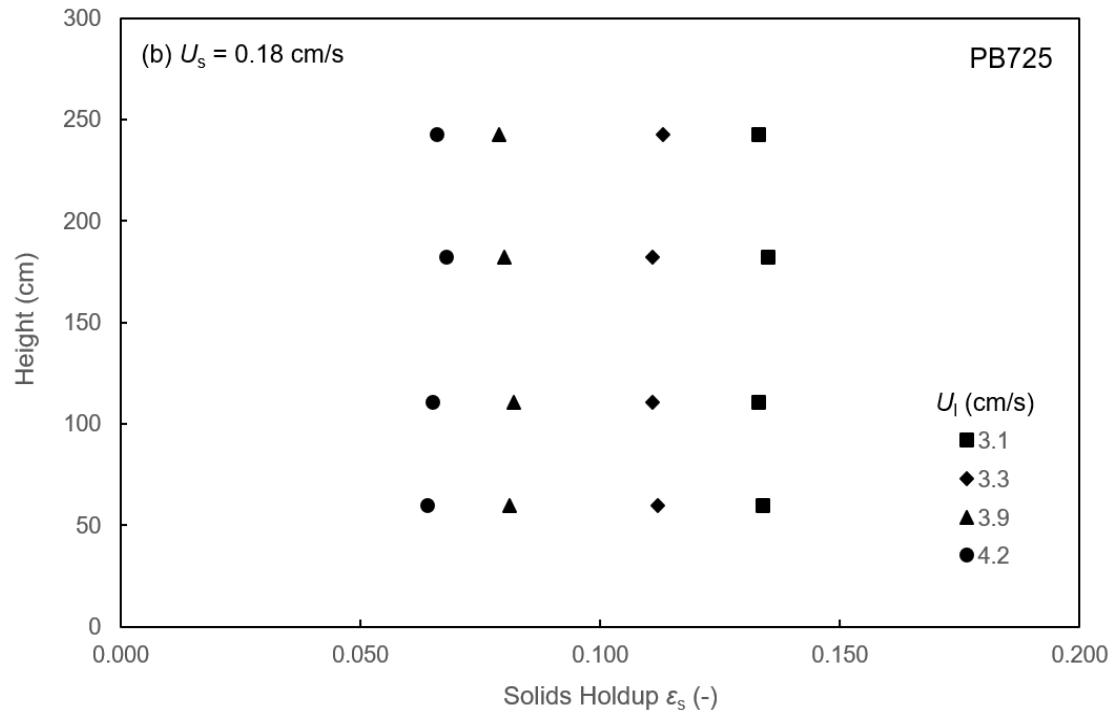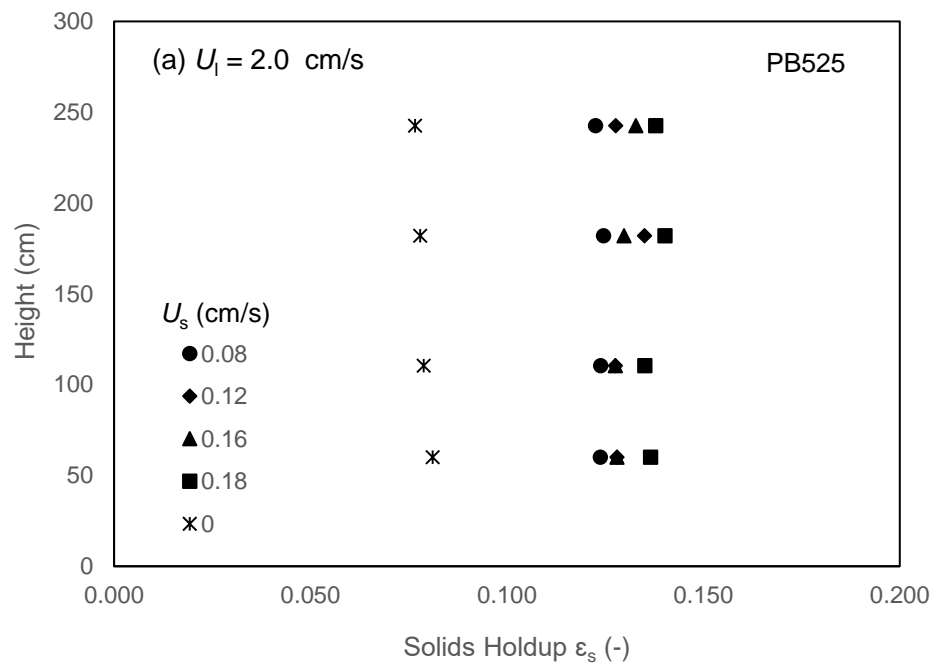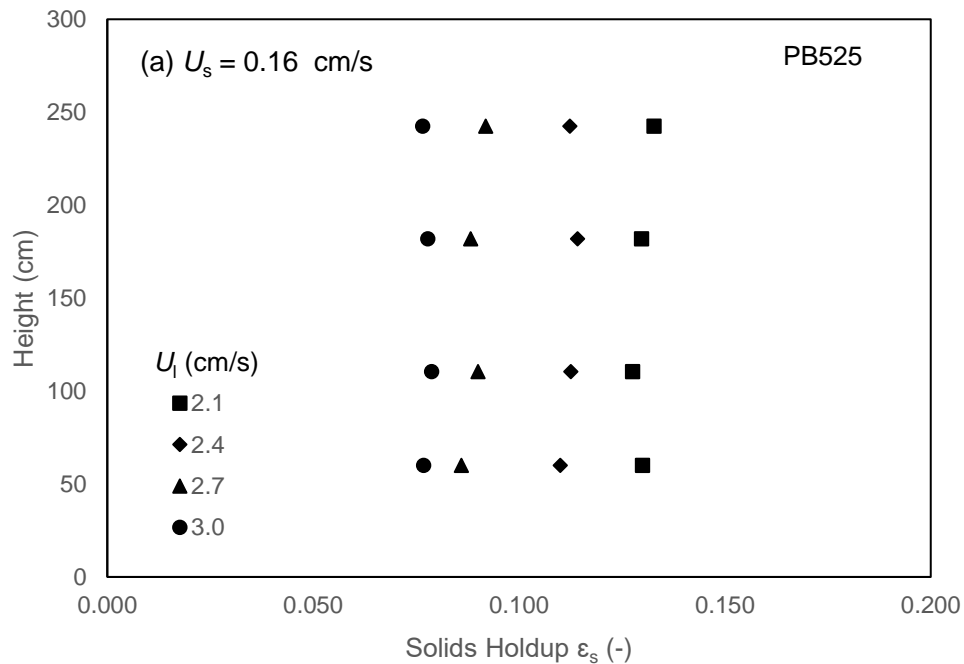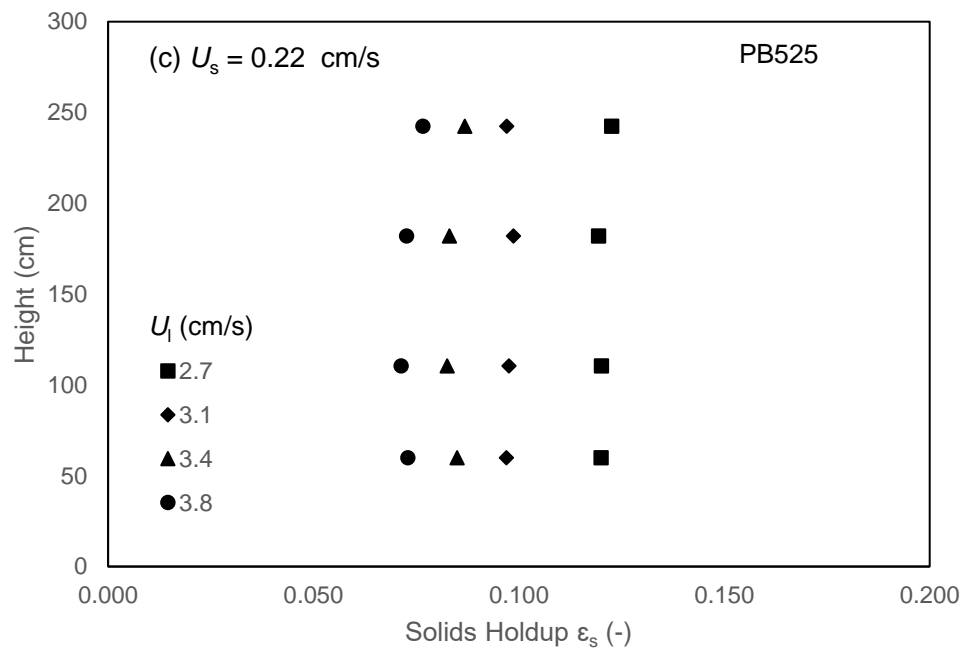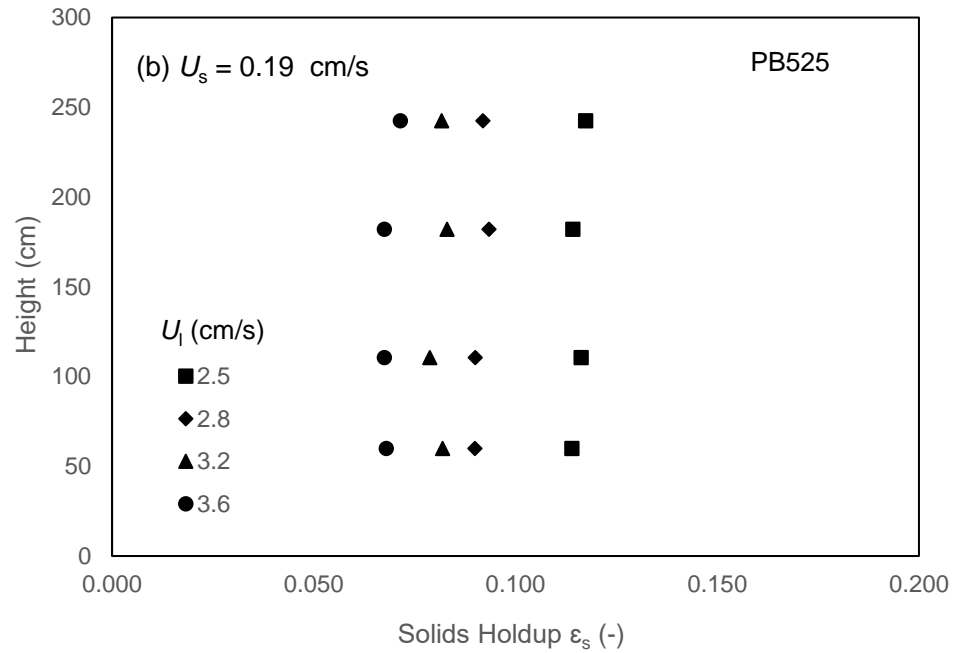
Figure 4.5 Axial solids holdup distribution for PB525 under different solids circulation rate (U_s) (a) 0.16 cm/s, (b) 0.19 cm/s and (c) 0.22 cm/s

The axial solids holdup distribution for PB525 under three different constant solids circulation rates, 0.16 cm/s, 0.19 cm/s and 0.22 cm/s, with varying superficial liquid velocities is shown in Figure 4.5. The data was collected at four different axial locations along the riser column by manometers. For a constant solids circulation rate, solids holdup decreases with the increasing superficial liquid velocity. Axial solids holdup distribution has the uniform trend under the different conditions.
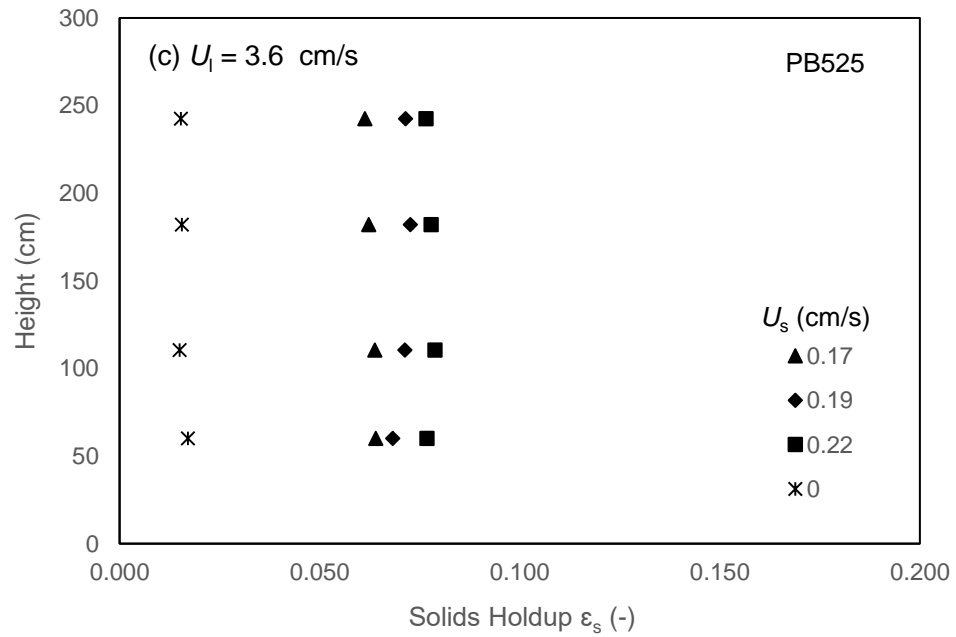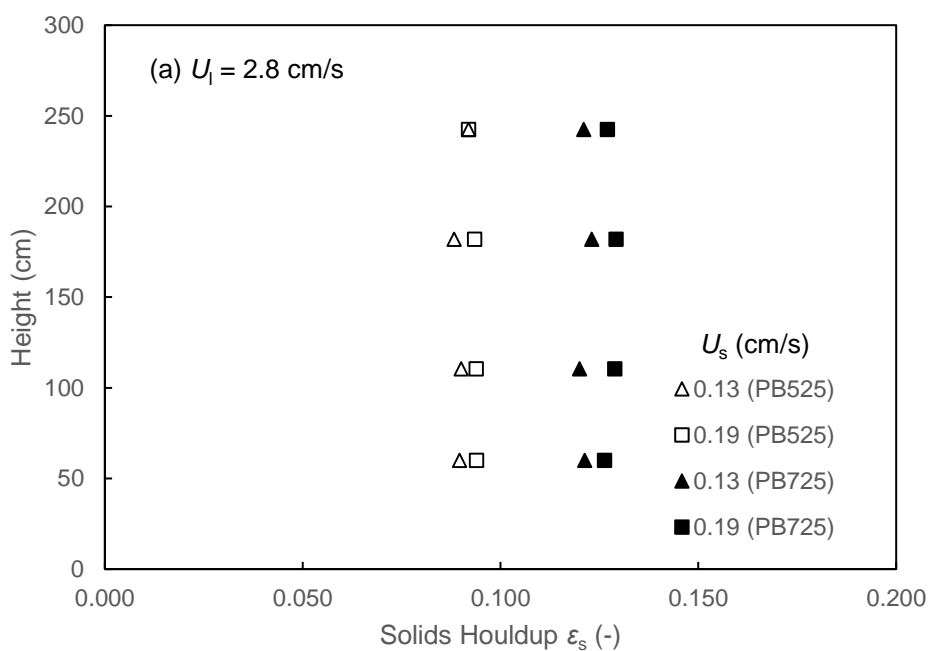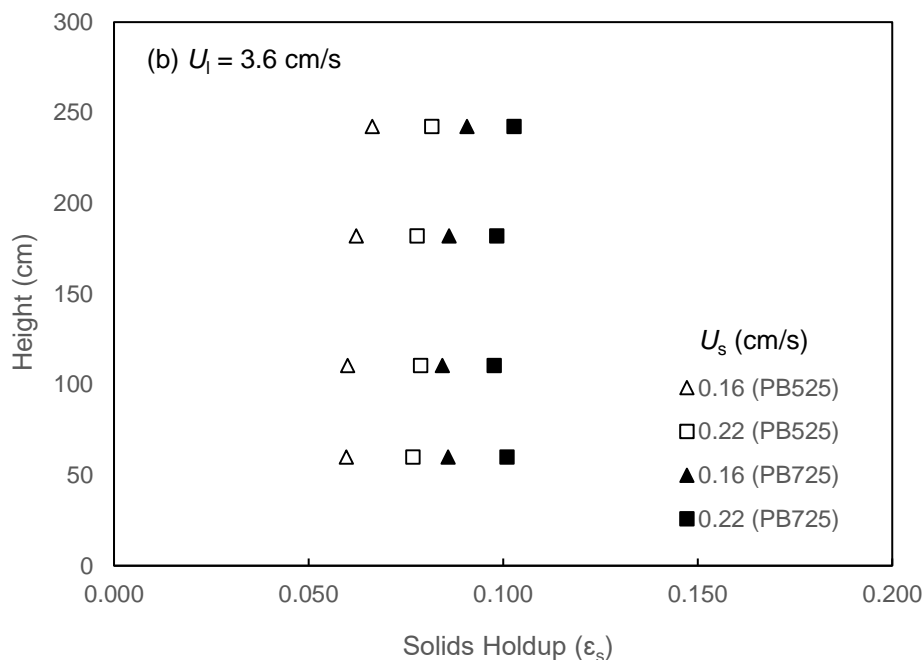
Figure 4.6 Axial solids holdup distribution for PB525 and PB725 under different superficial liquid velocity (U_l) (a) 2.8 cm/s and (b) 3.6 cm/s

Axial solids holdup distribution in CCFB for two types of particles, PB525 and Pb725, at constant superficial liquid velocities and varying solids circulation rate is presented in Figure 4.6. Under similar operating conditions, PB525 has less solids holdup than PB725. Because PB525 has less particle terminal velocity than PB725, that requires less energy to fluidize. With increasing solids circulation rate, axial solids holdup become more uniform for both types of particles.
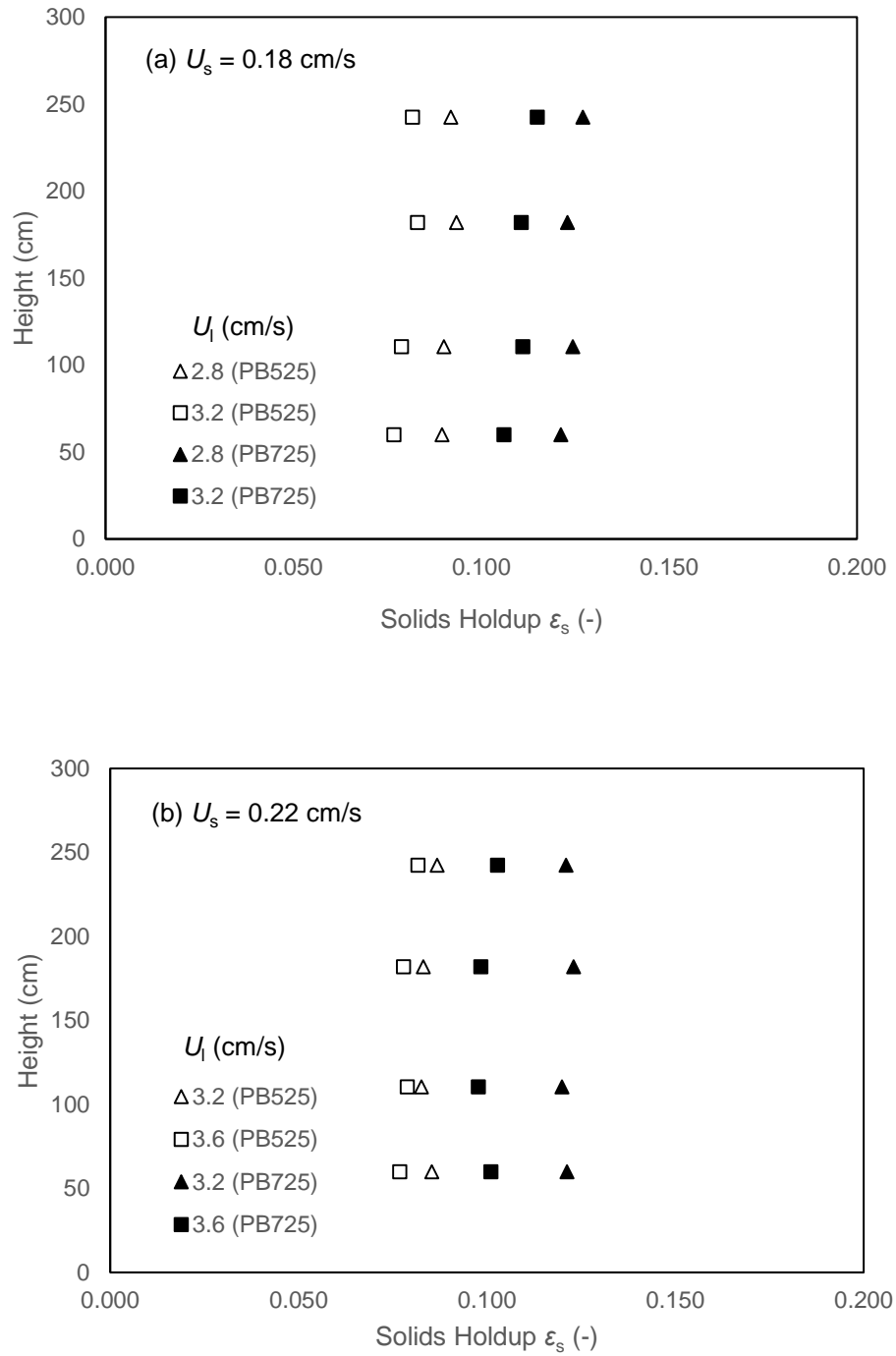
Figure 4.7 Axial solids holdup distribution for PB525 and PB725 under different solids circulation rate (U_s) (a) 0.18 cm/s and (b) 0.22 cm/s

The comparison of axial solids holdup distribution between PB525 and PB725 under different solids circulation rate is shown in Figure 4.7. At 0.18 cm/s solids circulation rate, the solids holdup of PB525 and PB725 was measured under 2.8 cm/s and 3.2 cm/s superficial liquid velocity, respectively. At 0.22 cm/s solids circulation rate, the solids holdup was taken under 3.2 cm/s and 3.6 cm/s superficial liquid velocity. At the similar operating conditions, PB725 had higher solids holdup than PB525.
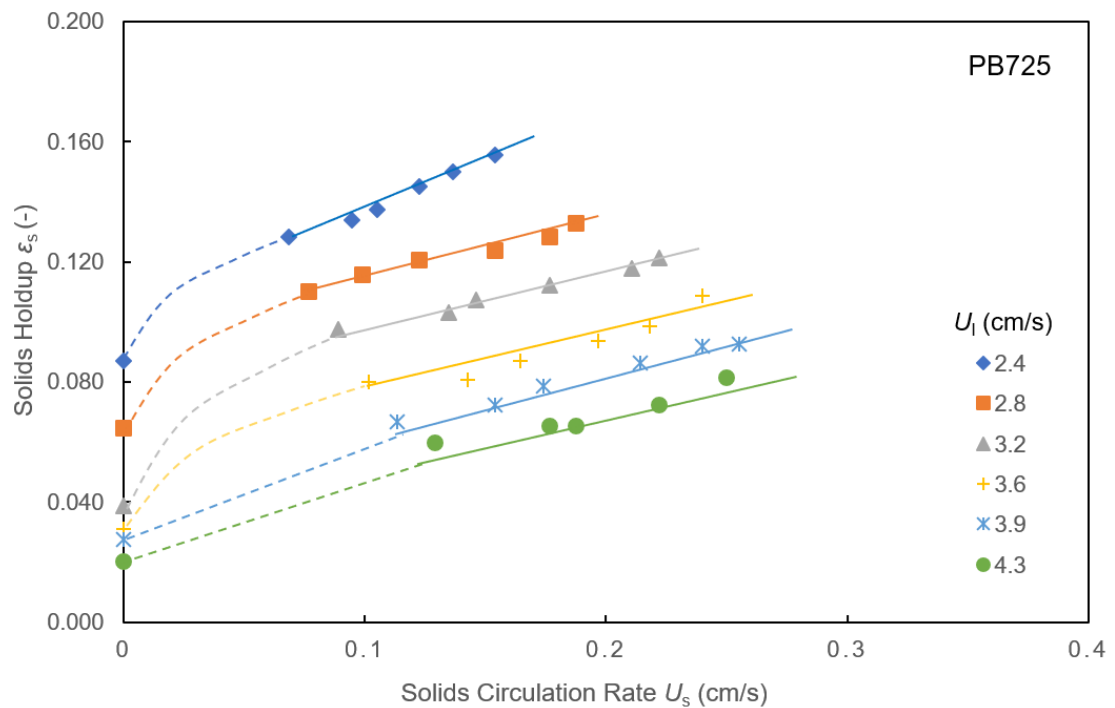
Figure 4.8 Solids holdup (ε_s) against solids circulation rate (U_s) under different superficial liquid velocity (U_l) for PB725
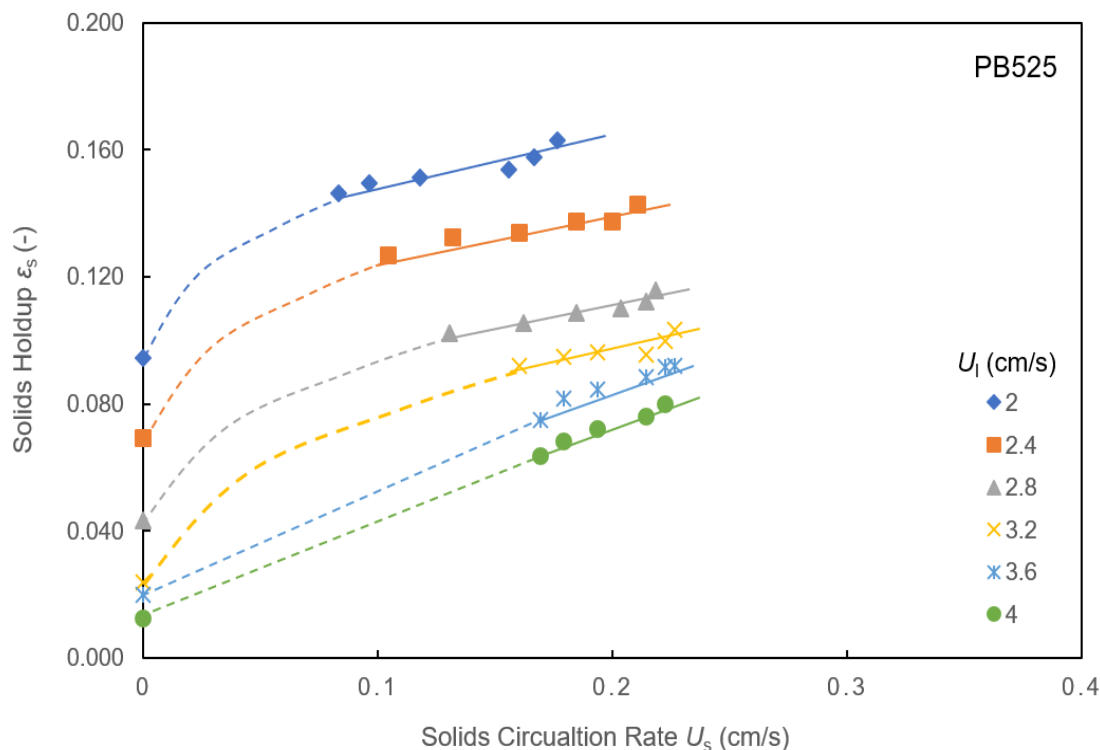
Figure 4.9 Solids holdup (ε_s) against solids circulation rate (U_s) under different superficial liquid velocity (U_l) for PB525

Figures 4.8 and 4.9 show the relationship between the average solids holdup and the solids circulation rate under different superficial liquid velocities for PB725 and PB525, respectively. The experiments of PB725 was operated under superficial liquid velocity increasing from 2.4 cm/s to 4.3 cm/s. For PB525, the experiment was operated under superficial liquid velocity increasing from 2.0 cm/s to 4.0 cm/s. The data on solids holdup were collected within conventional fluidization regime and within the conventional circulating fluidization regime. The dash line for each condition is a predicted trend line since in this interval, the solids circulation rate was very small and different to be controlled at an accurate value. The solids circulation rate was measured by butterfly valve but closing butterfly valve for a long time will affect the steady state of the system. From these trend lines, solids holdup increased with the increase of solids circulation

rate. With the increase of superficial liquid velocity, a more linear relationship between solids holdup and solids circulation rate was found.
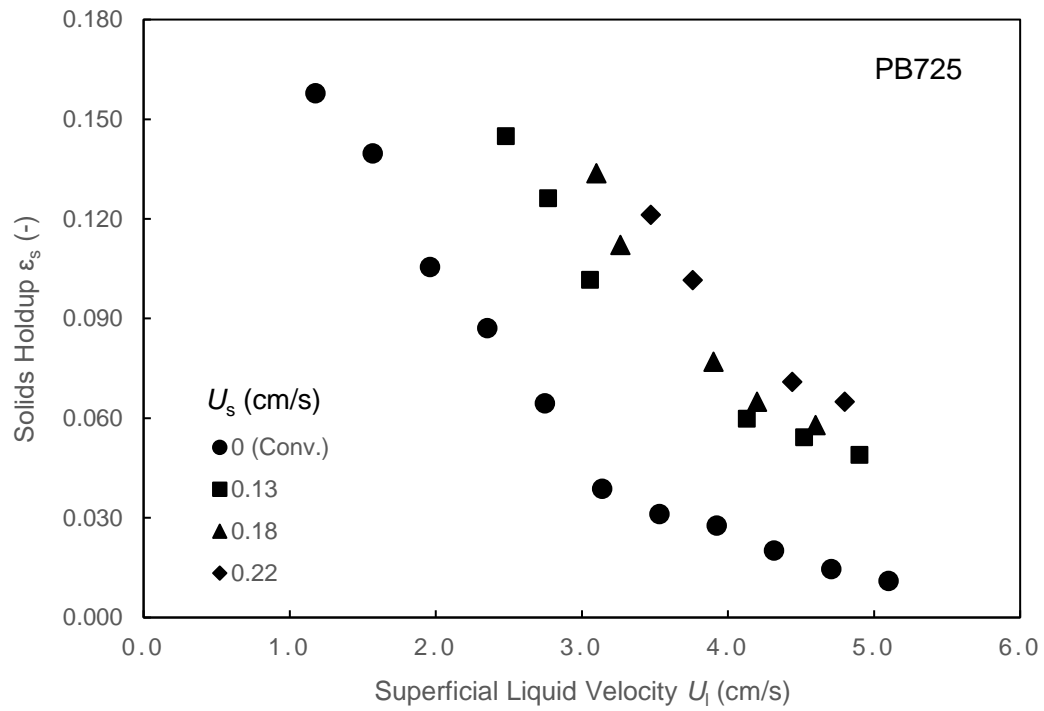
Figure 4.10 Solids holdup (ε_s) against superficial liquid velocity (U_l) under different solids circulation rate (U_s) for PB725
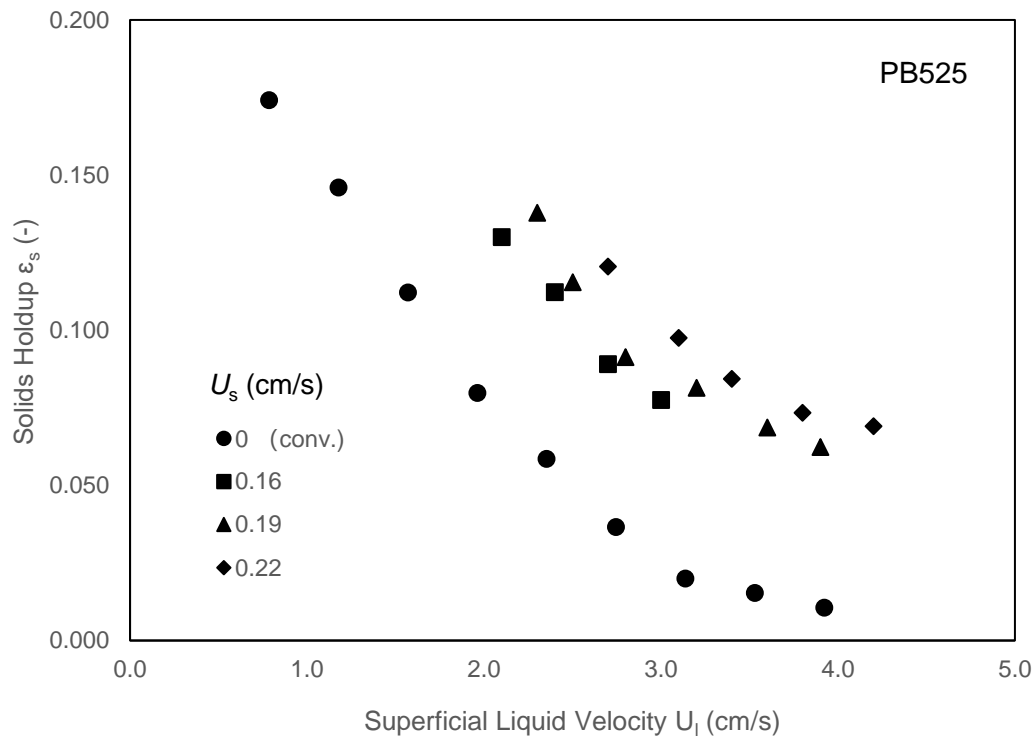
Figure 4.11 Solids holdup (ε_s) against superficial liquid velocity (U_l) under different solids circulation rate (U_s) for PB525

Figures 4.10 and 4.11 show the relationship between solids holdup and superficial liquid velocity under different solids circulation rate for PB725 and PB525, respectively. In conventional fluidization, solids holdup decreased sharply with superficial liquid velocity until particle terminal velocity and solids holdup reached zero. And CCFB find its place above conventional fluidization, since solids holdup is increased under each superficial liquid velocity by adding solids. Compared to the conventional fluidization, the solids holdup in conventional circulating fluidization is always higher than that in conventional fluidization which means higher solid-liquid contact efficiency in conventional circulating fluidization than conventional fluidization. For a liquid velocity, there is a corresponding solids holdup to balance the drag force and net gravity forces exerted on the particles. If extra particles are fed into an existing suspension, a transient higher solids

holdup condition is created, thus actual liquid velocity around particles increase, which lead to a higher drag force than net gravity force. The higher solids holdup condition cannot be maintained, as the forces are no longer balanced making the particles to be further suspended giving more room to liquid, thus drag force is reduced adapting net gravity force. Eventually, some solids are transported to a higher position due to the extra particles feed into the system while maintain constant liquid velocity. Under the same superficial liquid velocity, the solids holdup increases with the increasing of solids circulation rate.

4.3   Fluidized Bed Voidage verse Richardson – Zaki Equation

Richard-Zaki equation has been commonly used to predict bed voidage (or solids holdup) under particulate fluidization, in the conventional fluidization regime. The most basic form of the Richardson-Zaki equation is as follow:

$$\frac{U_l}{U_t} = \varepsilon_l^n \tag{4.1a}$$

or
$$\ln(\frac{U_l}{U_t}) = n \ln(\varepsilon_l) \tag{4.1b}$$

The theoretical value of parameter n can be calculated using the recommended values by Richardson and Zaki (Richardson & Zaki, 1954).

For $Re_t < 0.2$, $n = 4.65 + 19.5 d/D$.

For $0.2 < Re_t < 1$, $n = (4.35 + 17.5 d/D) Re_t^{-0.03}$.

For $1 < Re_t < 200$, $n = (4.45 + 18 d/D) Re_t^{-0.1}$.

For $200 < Re_t < 500$, $n = 4.45 Re_t^{-0.1}$ (Richardson & Zaki, 1954).

The terminal velocities for PB525 and PB725 are 5.6 and 8.8 cm/s, and terminal Reynolds numbers for PB525 and PB725 are 25 and 56, respectively. Accordingly, the corresponding theoretical values of parameter n are 3.44 and 3.25, theoretically, for PB525 and PB725 respectively, for conventional fluidization.

Figure 4.12 shows the relationship between $\ln(U_l/U_t)$ and $\ln(\varepsilon_l)$ for PB525 and PB725 in the conventional fluidization. The experimental values of parameter n were found to be 6.53 and 8.00 for PB525 and PB725 respectively. Those values, however, are much larger than the theoretical values of 3.44 and 3.25, as recommended by Richardson-Zaki equation.
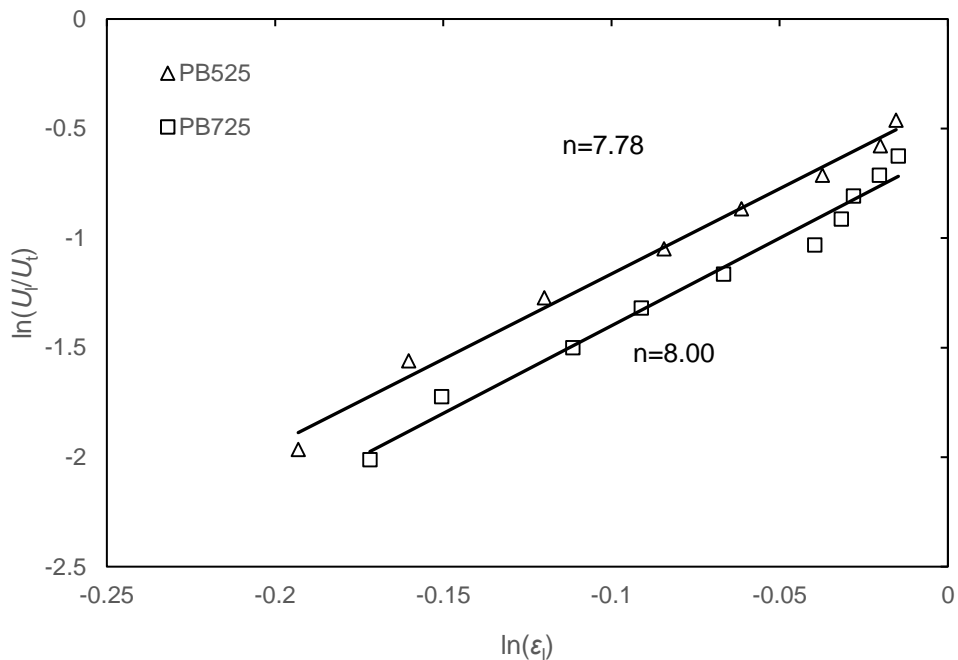
Figure 4.12 Relationship between $\ln(U_l/U_t)$ and $\ln(\varepsilon_l)$ for PB525 and PB725 in conventional fluidization

In principle, the Richard-Zaki equation can also be extended to predict the solids holdup in CCFB, with the inclusion of the solids circulation rate as shown by the following equation:

$$\frac{U_l}{\varepsilon_l} - \frac{U_s}{\varepsilon_s} = U_t \varepsilon_l^{n-1} \tag{4.2a}$$

or
$$\ln\left(\frac{U_{slip}}{U_t}\right) = (n-1)\ln(\varepsilon_l) \tag{4.2b}$$

The above relationship links the solids holdup with the slip velocity and the exponent n. Therefore, from the measured experimental bed expansion at different operating conditions, the actual exponent n can be estimated.

Figures 4.13 and 4.14 shows the relationship between $\ln(U_{slip}/U_t)$ and $\ln(\varepsilon_l)$ for PB525 and PB725 in the conventional circulating fluidized bed. By comparing to the conventional fluidization, it is worth noting that conventional circulating fluidization had a higher exponent n value for the Richardson-Zaki equation. Exponent n for PB525 has increased from 3.44 to 3.49 and that of PB725 has increased from 3.25 to 3.38. Therefore, the higher exponent n in CCFB when compared to conventional fluidized bed demonstrates that particles were in a more compact state in the CCFB, which also explained the higher solids holdup in the CCFB. It is believed that particle-particle interaction was intensified in the CCFB.
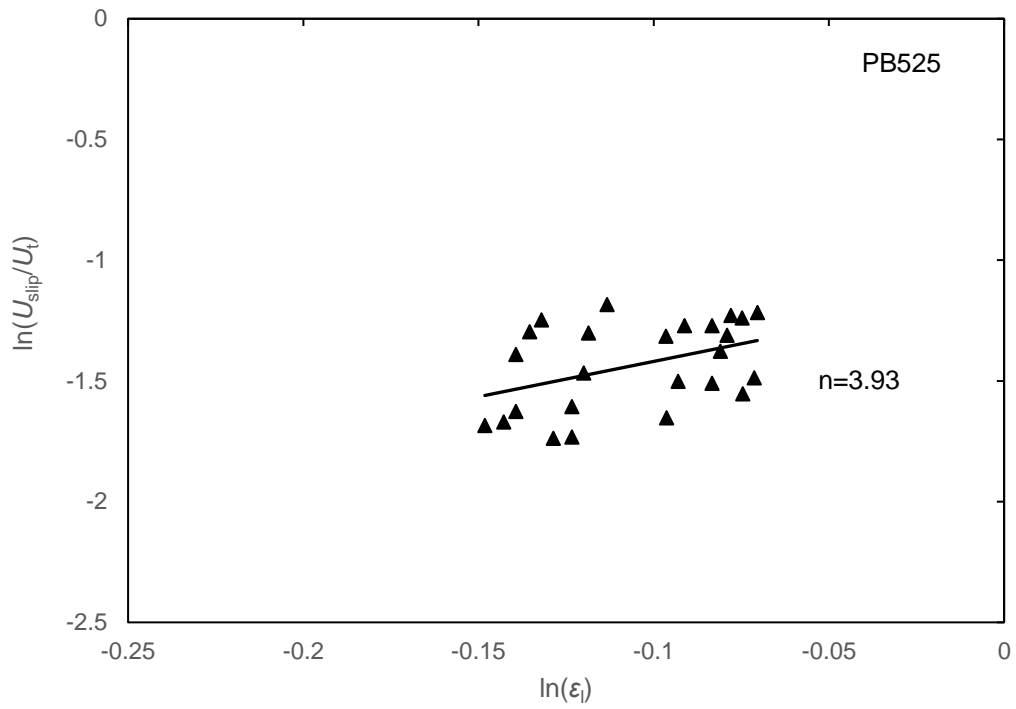
Figure 4.13 Relationship between ln(U_{slip}/U_t) and ln(ε_l) for PB525 in the CCFB
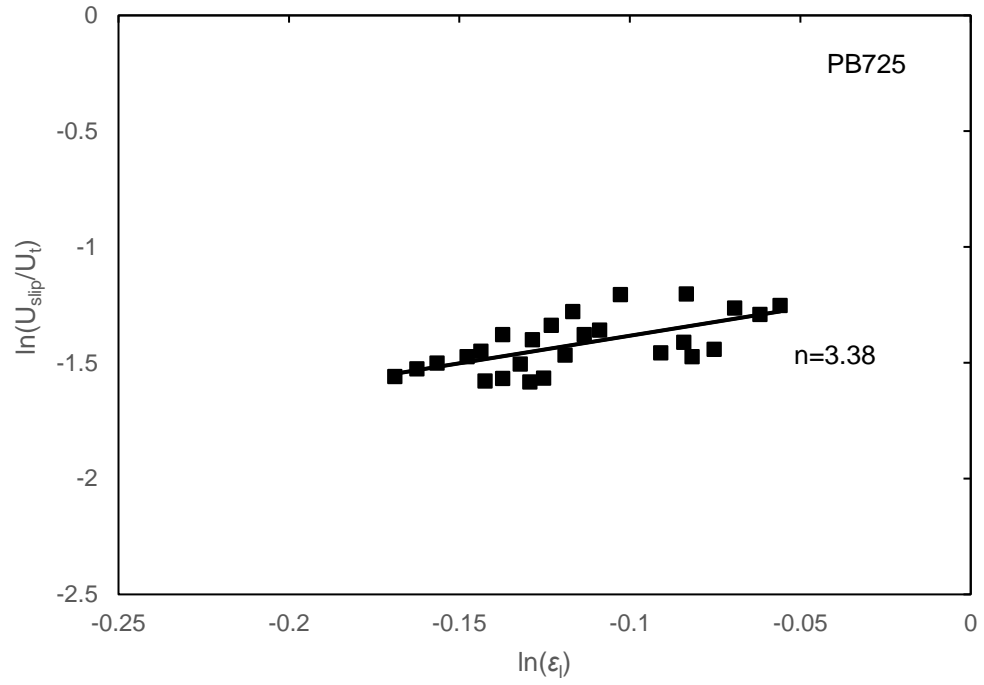
Figure 4.14 Relationship between ln(*U*slip/*U*t) and ln(*ε*l) for PB725 in the CCFB

Chapter 5

5 Conclusions and Recommendations

5.1 Conclusions

The concept of conventional circulating fluidized bed (CCFB) was proposed by combining a conventional fluidized bed (LSFB) and imposing external solids circulation as that in circulating fluidized bed (LSCFB). The hydrodynamics of the CCFB was investigated, by measuring the solids holdup at different operating conditions for two types of particles. The effects of particle properties, superficial liquid velocity and solids circulation rate were studied. Solids holdup was found to decrease with superficial liquid velocity and increase with solids circulation rate. Particles with higher density had lower solids holdup because of its lower particle terminal velocity. The axial solids holdup distribution was studied under a wide range of superficial liquid velocities and solids circulation rates. It was found that the increase of solids circulation rate resulted in more uniform distribution of solid in the axial direction of CCFB.

Compared to conventional liquid-solid fluidized bed (LSFB), the CCFB could reach higher solids holdup under the same superficial liquid velocity. The particle-particle interaction was increased in the CCFB due to the higher exponent n in Richardson-Zaki equation compared to that in conventional fluidized beds.

5.2 Recommendations for Future Work

In this research, only two types of particles were used, and they have different density and size. Another set of tests with two sizes of glass beads were planned but was not materialized due to Covid-19. The future work about the conventional circulation fluidization can focus on more particle properties, such as different materials, densities and sizes. It is necessary to adopt particles with common properties for accurate comparison on the effects of the individual properties. In addition, more hydrodynamic

characteristics could be investigated for the CCFB such as local solids holdup and local particle velocity. In brief, more work is essential for a more completely understanding of the hydrodynamics for potential applications about this novel CCFB.

Nomenclature

Ar	Archimedes number defined by $d_p^3 g(\rho_p - \rho_l)\rho^l/\mu_l^2$ (-)
C_D	Particle drag coefficient (-)
d_p	Particle diameter (µm)
d_p^*	Dimensionless Particle diameter (-)
g	Gravity acceleration (m/s^2)
Re	Reynolds number defined by $U_l d_p \rho_l/\mu_l$ (-)
Re_t	Terminal Reynolds number defined by $U_0 d_p \rho_l/\mu_l$ (-)
U^*	Dimensionless particle velocity (-)
U_0	Terminal falling velocity (cm/s)
U_a	Auxiliary liquid velocity (cm/s)
U_l	Superficial liquid velocity (cm/s)
U_s	Superficial solids velocity (cm/s)
U_{slip}	Slip velocity (cm/s)
U_t	Particle terminal velocity (cm/s)
U_{tr}	Transition velocity demarcate the conventional particulate regime and circulating fluidization regime (cm/s)

Greek letters

ε_s Solids holdup (-)

μ_l Liquid viscosity (mPa·s)

ρ_p Particle density (kg/m^3)

Subscripts

l Liquid

p Particle

s Solids

Abbreviation

LSFB   Conventional (low velocity) Liquid-Solid Fluidized Bed

LSCFB   Liquid-Solid Circulating (high velocity) Fluidized Bed

CCFB   Conventional Circulating Fluidized Bed

Reference

Anantharaman, A., Cocco, R. A., & Chew, J. W. (2018). Evaluation of Correlations for Minimum Fluidization Velocity (Umf) in Gas-Solid Fluidization. *Powder Technology, 323*, 454-485.

Atta, A., Razzak, S. A., Nigam, K. D. P., & Zhu, J.-X. (2009). (Gas)-Liquid-Solid Circulating Fluidized Bed Reactors: Characteristics and Applications. *Industrial and Engineering Chemistry Research, 48*(17), 7876-7892.

Babu, S. P., Shah, B., & Talwalkar, A. (1978). Fluidization Correlations for Coal Gasification Materials - Minimum Fluidization Vcelocity and Fluidized Bed Expansion Ratio. *AIChE Symposium Series, 74*(176), 176-186.

Bourgeois, P., & Grenier, P. (1968). The Ratio of Terminal Velocity to Minimum Fluidising Velocity for Spherical Particles. *The Canadian Journal of Chemical Engineering, 46*(5), 325-328.

Brereton, C. M. H., & Grace, J. R. (1993). Microstructural Aspects of the Behaviour of Circulating Fluidized Beds. *Chemical Engineering Science, 48*(14), 2565-2572.

Chen, B. H., & Douglas, W. J. M. (1968). Liquid Hold-up and Minimum Fluidization Velocity in a Turbulent Contactor. *The Canadian Journal of Chemical Engineering, 46*(4), 245-249.

Cheng, Y., & Zhu, J.-X. (2005). Cfd Modelling and Simulation of Hydrodynamics in Liquid-Solid Circulating Fluidized Beds. *The Canadian Journal of Chemical Engineering, 83*(2), 177-185.

Cheng, Y., & Zhu, J.-X. (2008). Hydrodynamics and Scale-up of Liquid-Solid Circulating Fluidized Beds: Similitude Method Vs. Cfd. *Chemical Engineering Science, 63*(12), 3201-3211.

Chowdhury, N., Nakhla, G., & Zhu, J.-X. (2008). Load Maximization of a Liquid–Solid Circulating Fluidized Bed Bioreactor for Nitrogen Removal from Synthetic Municipal Wastewater. *Chemosphere, 71*(5), 807-815.

Cornelissen, J. T., Taghipour, F., Escudié, R., Ellis, N., & Grace, J. R. (2007). Cfd Modelling of a Liquid–Solid Fluidized Bed. *Chemical Engineering Science, 62*(22), 6334-6348.

Davidson, J. F., Clift, R., & Harrison, D. (1985). Fluidization. *Academic Press, London*.

Eldyasti, A., Chowdhury, N., Nakhla, G., & Zhu, J.-X. (2010). Biological Nutrient Removal from Leachate Using a Pilot Liquid-Solid Circulating Fluidized Bed Bioreactor (Lscfb). *Journal of Hazardous Materials, 181*(1-3), 289-297.

Epstein, N. (2002). Applications of Liquid-Solid Fluidization. *International Journal of Chemical Reactor Engineering, 1*(1).

Fouda, A. E., & Capes, C. E. (1976). Calculation of Large Numbers of Terminal Velocities or Equivalent Particle Diameters Using Polynomial Equations Fitted to the Heywood Tables. *Powder Technology, 13*(2), 291-293.

Geldart, D. (1973). Types of Gas Fluidization. *Powder Technology, 7*(5), 285-292.

Geldart, D. (1986). Gas Fluidization Technology. *Wiley, New York*.

Grace, J. R. (1986). Contacting Modes and Behaviour Classification of Gas-Solid and Other Two-Phase Suspensions. *The Canadian Journal of Chemical Engineering, 64*(3), 353-363.

Haider, A., & Levenspiel, O. (1989). Drag Coefficient and Terminal Velocity of Spherical and Non-Spherical Particles. *Powder Technology, 58*(1), 63-70.

Happel, J., & Brenner, H. (1973). Low Reynolds Number Hydrodynamics. *Martinus Nijhoff, Hague*.

Hartman, M., Trnka, O., & Svoboda, K. (1994). Free Settling of Nonspherical Particles. *Industrial and Engineering Chemistry Research, 33*(8), 1979-1983.

Jean, R.-H., & Liang-Shin, F. (1989). A Fluid Mechanic-Based Model for Sedimentation and Fluidization at Low Reynolds Numbers. *Chemical Engineering Science, 44*(2), 353-362.

Kalaga, D. V., Dhar, A., Dalvi, S. V., & Joshi, J. B. (2014). Particle-Liquid Mass Transfer in Solid-Liquid Fluidized Beds. *Chemical Engineering Journal, 245*(323-341).

Karamanev, D. G. (1996). Equations for Calculation of the Terminal Velocity and Drag Coefficient of Solid Spheres and Gas Bubbles. *Chemical Engineering Communications, 147*, 75-84.

Kwauk, M. (1963). Generalized Fluidization I.Steady-State Motion. *Scientia Sinica, 12*(4), 587-612.

Kwauk, M. (1992). Fluidization: Idealized and Bubbleless, with Applications. *Ellis horwood, New York*.

Kwauk, M., Li, J., & Liu, D. (2000). Particulate and Aggregative Fluidization - 50 Years in Retrospect. *Powder Technology, 111*(1-2), 3-18.

Lan, Q., Zhu, J.-X., Bassi, A., Margaritis, A., Zheng, Y., & Rowe, G. E. (2000). Continuous Protein Recovery Using a Liquid–Solid Circulating Fluidized Bed Ion

Exchange System Modelling and Experimental Studies. *The Canadian Journal of Chemical Engineering, 78*(5), 858-866.

Leve, M. (1959). Fluidization. *McGraw-Hill. New York*.

Liang, W.-G., & Zhu, J.-X. (1997). A Core-Annulus Model for the Radial Flow Structure in a Liquid-Solid Circulating Fluidized Bed (Lscfb). . *Chemical Engineering Journal, 68*(1), 51-62.

Liang, W., Zhang, S., Yu, Z., Jin, Y., & Wu, Q. (1993). Liquid-Solid Circulating Fluidized Bed (I): Studies on the Phase Holdups and Solid Circulating Rate. *Huagong Xuebao/Journal of Chemical Industry and Engineering (China), 44*(6), 666-671.

Liang, W., Zhang, S., Zhu, J.-X., Jin, Y., Yu, Z., & Wang, Z. (1997). Flow Characteristicsof the Liquid–Solid Circulating Fluidized Bed. *Powder Technology, 90*(2), 95-102.

Lin, C.-L., Wey, M.-Y., & You, S.-D. (2002). The Effect of Particle Size Distribution on Minimum Fluidization Velocity at High Temperature. *Powder Technology, 126*(3), 297-301.

Lippens, B. C., & Mulder, J. (1993). Prediction of the Minimum Fluidization Velocity. *Powder Technology, 75*(1), 67-78.

Lucas, A., Arnaldos, J., Casal, J., & Pulgjaner, L. (1986). Improved Equation for the Calculation of Minimum Fluidization Velocity. *Industrial and Engineering Chemistry Process Design and Development, 25*(2), 426-429.

Miura, H., Takahashi, T., Ichikawa, J., & Kawase, Y. (2001). Bed Expansion in Liquid-Solid Two-Phase Fluidized Beds with Newtonian and Non-Newtonian Fluids over the Wide Range of Reynolds Numbers. *Powder Technology, 117*(3), 239-246.

Mori, S., & Wen, C. Y. (1975). Estimation of Bubble Diameter in Gaseous Fluidized Beds. *AIChE Journal, 21*(1), 109-115.

Nelson, M. J., Nakhla, G., & Zhu, J.-X. (2017). Fluidized-Bed Bioreactor Applications for Biological Wastewater Treatment: A Review of Research and Developments. *Engineering, 3*(3), 330-342.

Palani, N., Ramalingam, V., Ramadoss, G., & Seeniraj, R. V. (2011). Study of Slip Velocity and Application of Drift-Flux Model to Slip Velocity in a Liquid-Solid Circulating Fluidized Bed. *Advanced Powder Technology, 22*(1), 77-85.

Palani, N., Velraj, R., & Seeniraj, R. V. (2007). A Model to Predict Radial Solids Holdup and Liquid Velocity Distributions in Liquid-Solid Circulating Fluidized Bed. *Chemical Product and Process Modeling, 2*(3).

Patel, A., Zhu, J.-X., & Nakhla, G. (2006). Simultaneous Carbon, Nitrogen and Phosphorous Removal from Municipal Wastewater in a Circulating Fluidized Bed Bioreactor. *Chemosphere, 65*(7), 1103-1112.

Patel, M., Bassi, A. S., Zhu, J.-X., & Gomaa, H. (2008). Investigation of a Dual-Particle Liquid-Solid Circulating Fluidized Bed Bioreactor for Extractive Fermentation of Lactic Acid. *Biotechnology Progress, 24*(4), 821-831.

Razzak, S. A., Rahman, S. M., Hossain, M. M., & Zhu, J.-X. (2012). Investigation of Artificial Neural Network Methodology for Modeling of a Liquid-Solid Circulating Fluidized Bed Riser. *Powder Technology, 229*, 71-77.

Reh, L. (1971). Fluidized Bed Processing. *Chemical Engineering Progress, 67*(2), 58-63.

Richardson, J. F., & da S. Jerónimo, M. A. (1979). Velocity-Voidage Relations for Sedimentation and Fluidisation. *Chemical Engineering Science, 34*(12), 1419-1422.

Richardson, J. F., & Zaki, W. N. (1954). Sedimentation and Fluidisation: Part I. *Transactions of the Institution of Chemical Engineers, 32*, 35-53.

Roy, S., Chen, J., Kumar, S. B., Al-Dahhan, M. H., & Duduković, M. P. (1997). Tomographic and Particle Tracking Studies in a Liquid-Solid Riser. *Industrial and Engineering Chemistry Research, 36*(11), 4666-4669.

Roy, S., & Dudukovic, M. (2001). Flow Mapping and Modeling of Liquid-Solid Risers. *Industrial and Engineering Chemistry Research, 40*(23), 5440-5454.

Roy, S., Kemoun, A., Al-Dahhan, M. H., & Dudukovic, M. P. (2005). Experimental Investigation of the Hydrodynamics in a Liquid-Solid Riser. *AIChE Journal, 51*(3), 802-835.

Sang, L., & Zhu, J.-X. (2012). Experimental Investigation of the Effects of Particle Properties on Solids Holdup in a Lscfb Riser. *Chemical Engineering Journal, 197*, 322-329.

Saxena, S. C., & Vogel, G. J. (1977). Measurement of Incipient Fluidisation Velocities in a Bed of Coarse Dolomite at Temperature and Pressure. *Transactions of the Institution of Chemical Engineers, 55*(3), 184-189.

Tavoulareas, S. (1991). Fluidized-Bed Combustion Technology. *Annual Review of Energy and the Environment, 116*, 25-57.

Thonglimp, V., Hiquily, N., & Laguerie, C. (1984). Minimum Fluidization Speed and Expansion of the Layers of Mixtures of Solid Particles Fluidized by a Gas. *Powder Technology, 39*(2), 223-239.

Trivedi, U., Bassi, A., & Zhu, J.-X. (2006). Continuous Enzymatic Polymerization of Phenol in a Liquid–Solid Circulating Fluidized Bed. *Powder Technology, 169*(2), 61-70.

Wen, C. Y., & Yu, Y. H. (1966). A Generalized Method for Predicting the Minimum Fluidization Velocity. *AIChE Journal, 12*(3), 610-612.

Werther, J., & Molerus, O. (1973). The Local Structure of Gas Fluidized Beds -Ii. The Spatial Distribution of Bubbles. *International Journal of Multiphase Flow, 1*(1), 123-138.

Wilhelm, R. H., & Kwauk, M. (1948). Fluidization of Solid Particles. *Chemical Engineering Progress, 44*, 201-218.

Yang, W. (2003). Handbook of Fluidization and Fluid–Particle System. *Marcel Dekker, New York*.

Yerushalmi, J., Graff, R. A., Squires, A. M., & Dobner, S. (1976). Production of Gaseous Fuels from Coal in the Fast Fluidized Bed. *Fluidization Technology, 2*, 437-469.

Zhang, H., Wang, T., & Wang, J. (2003). Particle Velocity Field in Liquid-Solid Circulating Fluidized Beds. *Huagong Xuebao/Journal of Chemical Industry and Engineering (China), 54*(10), 1355-1360.

Zheng, Y., & Zhu, J.-X. (2000a). Microstructural Aspects of the Flow Behaviour in a Liquid-Solids Circulating Fluidized Bed. *The Canadian Journal of Chemical Engineering, 78*(1), 75-81.

Zheng, Y., & Zhu, J.-X. (2000b). Overall Pressure Balance and System Stability in a Liquid–Solid Circulating Fluidized Bed. *Chemical Engineering Journal, 79*(2), 145-153.

Zheng, Y., & Zhu, J.-X. (2002). Radial Distribution of Liquid Velocity in a Liquid-Solids Circulating Fluidized Bed. *International Journal of Chemical Reactor Engineering, 1*(1).

Zheng, Y., Zhu, J.-X., Wen, J., Martin, S. A., Bassi, A. S., & Margaritis, A. (1999). The Axial Hydrodynamic Behavior in a Liquid-Solid Circulating Fluidized Bed. *The Canadian Journal of Chemical Engineering, 77*(2), 284-290.

Zhu, J.-X., Zheng, Y., Karamanev, D. G., & Bassi, A. S. (2000). (Gas-)Liquid-Solid Circulating Fluidized Beds and Their Potential Applications to Bioreactor Engineering. *The Canadian Journal of Chemical Engineering, 78*(1), 82-94.

Appendices

Appendix A. Average Solids Holdup Data of Each Particles

Appendix 1 Average solids holdup data of PB725

U_l (cm/s)	U_s (cm/s)	ε_s	U_l (cm/s)	U_s (cm/s)	ε_s
2.4	0.07	0.128	3.9	0.11	0.067
2.4	0.09	0.134	3.9	0.15	0.072
2.4	0.11	0.137	3.9	0.17	0.078
2.4	0.12	0.145	3.9	0.21	0.086
2.4	0.14	0.150	3.9	0.24	0.092
2.4	0.15	0.155	3.9	0.26	0.093
2.8	0.08	0.110	4.3	0.13	0.060
2.8	0.10	0.116	4.3	0.18	0.065
2.8	0.12	0.121	4.3	0.19	0.065
2.8	0.15	0.124	4.3	0.22	0.072
2.8	0.18	0.128	4.3	0.25	0.081
2.8	0.19	0.133	4.3	0.26	0.085
3.2	0.09	0.098	4.7	0.13	0.054
3.2	0.13	0.103	4.7	0.18	0.058
3.2	0.15	0.107	4.7	0.20	0.060
3.2	0.18	0.112	4.7	0.22	0.065
3.2	0.21	0.118	4.7	0.25	0.067
3.2	0.22	0.121			
3.6	0.10	0.080			
3.6	0.14	0.081			
3.6	0.16	0.087			
3.6	0.20	0.094			
3.6	0.22	0.098			
3.6	0.24	0.109			

Appendix 2 Average solids holdup data of PB525

U_l (cm/s)	U_s (cm/s)	ε_s	U_l (cm/s)	U_s (cm/s)	ε_s
2.0	0.08	0.146	3.2	0.16	0.092
2.0	0.10	0.149	3.2	0.18	0.095
2.0	0.12	0.151	3.2	0.19	0.096
2.0	0.16	0.154	3.2	0.21	0.096
2.0	0.17	0.157	3.2	0.22	0.100
2.0	0.18	0.163	3.2	0.23	0.103
2.4	0.10	0.127	3.6	0.17	0.075
2.4	0.13	0.132	3.6	0.18	0.081
2.4	0.16	0.134	3.6	0.19	0.084
2.4	0.18	0.137	3.6	0.21	0.089
2.4	0.20	0.137	3.6	0.22	0.090
2.4	0.21	0.143	3.6	0.23	0.092
2.8	0.13	0.102	4.0	0.17	0.063
2.8	0.16	0.105	4.0	0.18	0.068
2.8	0.18	0.109	4.0	0.19	0.072
2.8	0.20	0.110	4.0	0.21	0.076
2.8	0.21	0.112	4.0	0.22	0.080
2.8	0.22	0.116			

Appendix B. Analytic Data of Exponent *n* in Conventional Fluidization

Appendix 3 Analytic data of exponent *n* of PB725 in conventional fluidization

U_l (cm/s)	U_t (cm/s)	ε_s	$\ln(U_l/U_t)$	$\ln(\varepsilon_l)$
1.2	8.8	0.158	-2.0120466	-0.17181
1.6	8.8	0.140	-1.7243645	-0.15053
2.0	8.8	0.106	-1.5012209	-0.11153
2.4	8.8	0.087	-1.3188994	-0.09114
2.7	8.8	0.065	-1.1647487	-0.06673
3.1	8.8	0.039	-1.0312173	-0.03962
3.5	8.8	0.031	-0.9134343	-0.03171
3.9	8.8	0.028	-0.8080738	-0.02811
4.3	8.8	0.020	-0.7127636	-0.02037
4.7	8.8	0.015	-0.6257522	-0.01473

Appendix 4 Analytic data for exponent *n* of PB525 in conventional fluidization

U_l (cm/s)	U_t (cm/s)	ε_s	$\ln(U_l/U_t)$	$\ln(\varepsilon_l)$
0.8	5.6	0.206	-1.9655266	-0.23078
1.2	5.6	0.173	-1.5600614	-0.18978
1.6	5.6	0.133	-1.2723794	-0.14239
2.0	5.6	0.094	-1.0492358	-0.09921
2.4	5.6	0.069	-0.8669143	-0.07182
2.7	5.6	0.043	-0.7127636	-0.04422
3.1	5.6	0.024	-0.5792322	-0.02394
3.5	5.6	0.018	-0.4614492	-0.01828

Appendix C. Analytic Data of Exponent *n* in Conventional Circulating Fluidization

Appendix 5 Analytic data of exponent *n* of PB725 in conventional circulating fluidization

U_l (cm/s)	U_s (cm/s)	ε_s	$\ln(U_{slip}/U_t)$	$\ln(\varepsilon_l)$
2.4	0.07	0.128	-1.37787	-0.13728
2.4	0.09	0.134	-1.44976	-0.14366
2.4	0.11	0.137	-1.47391	-0.14771
2.4	0.12	0.145	-1.50093	-0.15655
2.4	0.14	0.150	-1.52589	-0.16239
2.4	0.15	0.155	-1.55855	-0.16893
2.8	0.08	0.110	-1.27933	-0.11672
2.8	0.10	0.116	-1.33782	-0.12297
2.8	0.12	0.121	-1.40056	-0.12853
2.8	0.15	0.124	-1.50566	-0.13212
2.8	0.18	0.128	-1.56698	-0.13728
2.8	0.19	0.133	-1.57799	-0.14243
3.2	0.09	0.098	-1.20577	-0.10269
3.2	0.13	0.103	-1.35951	-0.10879
3.2	0.15	0.107	-1.37808	-0.11333
3.2	0.18	0.112	-1.46613	-0.11898
3.2	0.21	0.118	-1.56572	-0.12525
3.2	0.22	0.121	-1.58208	-0.12926
3.6	0.10	0.080	-1.20316	-0.0834
3.6	0.14	0.081	-1.41179	-0.08409
3.6	0.16	0.087	-1.4564	-0.09091
3.9	0.11	0.067	-1.26338	-0.06925
3.9	0.15	0.072	-1.44176	-0.07521
3.9	0.17	0.078	-1.47339	-0.08174
4.3	0.13	0.060	-1.29129	-0.06175
4.7	0.13	0.054	-1.25191	-0.05587
4.7	0.18	0.058	-1.49671	-0.06018

Appendix 6 Analytic data of exponent *n* of PB525 in conventional circulating fluidization

U_l (cm/s)	U_s (cm/s)	ε_s	$\ln(U_{slip}/U_t)$	$\ln(\varepsilon_l)$
2.0	0.16	0.154	-1.42195	-0.16709
2.0	0.17	0.157	-1.44856	-0.17136
2.0	0.18	0.163	-1.45498	-0.17796
2.4	0.18	0.137	-1.35981	-0.14771
2.4	0.20	0.137	-1.44095	-0.14771
2.4	0.21	0.143	-1.44032	-0.15416
2.8	0.18	0.109	-1.35622	-0.11505
2.8	0.20	0.110	-1.46011	-0.11672
2.8	0.22	0.116	-1.47533	-0.12297
3.2	0.18	0.095	-1.22695	-0.09941
3.2	0.19	0.096	-1.29979	-0.10105
3.6	0.17	0.075	-1.22906	-0.07796
3.6	0.18	0.081	-1.17947	-0.08501
3.6	0.19	0.084	-1.22995	-0.08812
4.0	0.18	0.068	-1.21718	-0.07042
4.0	0.19	0.072	-1.239	-0.07472

Curriculum Vitae

Name: Xinyu Pan

Post-secondary Education and Degrees: Zhejiang Normal University
Jinhua, Zhejiang, China
2013-2016

The University of Western Ontario
London, Ontario, Canada
2016-2018 B.E.Sc.
2018-2020 M.E.Sc.

Honours and Awards: The University of Western Ontario Graduate Research Scholarship
2018-2020

Related Work Experience Teaching Assistant
The University of Western Ontario
2019